Definition of the Cultana Subsuite, Gawler Craton: A high level felsic Hiltaba Suite age intrusive with hydrothermal alteration and brecciation

Stacey McAvaney

Report Book 2008/11

Government of South Australia
Primary Industries and Resources SA

080747

Definition of the Cultana Subsuite, Gawler Craton: A high level felsic Hiltaba Suite age intrusive with hydrothermal alteration and brecciation

Stacey McAvaney

Geological Survey Branch

September 2008

Report Book 2008/11

Government of South Australia
Primary Industries and Resources SA

Division of Minerals and Energy Resources
Primary Industries and Resources South Australia
7th floor, 101 Grenfell Street, Adelaide
GPO Box 1671, Adelaide SA 5001
Phone National (08) 8463 3204
International +61 8 8463 3204
Fax National (08) 8463 3229
International +61 8 8463 3229
Email pirsa.minerals@saugov.sa.gov.au
Website www.minerals.pir.sa.gov.au

Preferred way to cite this publication
McAvaney, S.O., 2008. Definition of the Cultana Subsuite, Gawler Craton: A high level felsic Hiltaba Suite age intrusive with hydrothermal alteration and brecciation. *South Australia. Department of Primary Industries and Resources. Report Book* 2008/11.

CONTENTS

TABLES

FIGURES

Definition of the Cultana Subsuite, Gawler Craton: A high level felsic Hiltaba Suite age intrusive with hydrothermal alteration and brecciation

Stacey McAvaney

INTRODUCTION

The Cultana Subsuite is a high level felsic magmatic intrusion located in the southeastern Gawler Craton, South Australia (Fig. 1) The subsuite is part of the Hiltaba Suite, an early Mesoproterozoic (c. 1595–1575 Ma) bimodal magmatic suite that is widespread across the Gawler Craton and coeval with the voluminous Gawler Range Volcanics (Flint et al., 1993; Creaser, 1996). The Cultana Subsuite comprises a range of comagmatic granitic and porphyritic lithologies, including quartz – feldspar porphyry, alkali granite, feldspar-phyric granophyric monzogranite, alkali feldspar microgranite and syeno-microgranite. It is exposed only in the Cultana Inlier (Fig.1).

The Cultana Subsuite is located within the Olympic Cu-Au-(U) Province (2003; Skirrow et al., 2006), which extends along the eastern Gawler Craton and hosts a number of iron oxide-copper-gold (IOCG) deposits and prospects, including Olympic Dam (Oreskes and Einaudi, 1990; Reeve et al., 1990; Haynes, 1995; Reynolds, 2001), Prominent Hill (Belperio and Freeman, 2004; Belperio et al., 2007), Oak Dam (Davidson et al., 2007), Acropolis and Wirrda Well (Daly et al., 1998), Moonta-Wallaroo (Conor, 1995) and Carrapateena (Fairclough, 2005) (Fig. 1). These deposits and prospects are hosted within a range of Palaeo- to Mesoproterozoic units, but are temporally and genetically associated with the Gawler Range Volcanics – Hiltaba Suite magmatic event (Skirrow et al., 2007).

Like these deposits and prospects, the Cultana Subsuite has been affected by iron – rich hydrothermal alteration, which locally occurs in the form of haematite-sericite-chlorite-quartz-tourmaline replacement and veining and haematite-rich brecciation. Unlike the deposits and prospects in the north of the Olympic Cu-Au-(U) Province which lie under cover of the Mesoproterozoic Cariewerloo Basin, Neoproterozoic Stuart Shelf or Phanerozoic sediments, the Cultana Subsuite is outcropping. It is exposed in the Cultana Inlier, a fault-bound block of Palaeoproterozoic to early Neoproterozoic rocks, which has been uplifted from beneath the cover (Fig. 2).

Only limited exploration has been carried out in the Cultana Inlier (summarised in App. 1), primarily due to the difficulties in land access. There are only three drill holes in the inlier, none of which intersect the Cultana Subsuite at depth. Serem Pty Ltd (1971) explored the inlier for copper porphyry mineralisation between 1970–71, drilling three holes in the vicinity of Old Point Lowly copper mine. Sibenaler (1972) from the Department of Mines assessed the tin potential of the intrusion as part of a wider study of South Australian granitoids. Both Normandy and Craton Resources (2001) explored the Cultana Inlier in the 1990s for IOCG-U mineralisation, and carried out rock chip and stream sediment sampling and geological mapping. Eagle Bay Resources and Minotaur Exploration are currently exploring in the Cultana inlier for IOCG mineralisation (Eagle Bay Resources, 2008).

This paper provides a formal definition of the Cultana Subsuite, outlining the igneous petrology of the intrusion, its geochemical characteristics, and the nature of hydrothermal alteration and brecciation affecting the rocks.

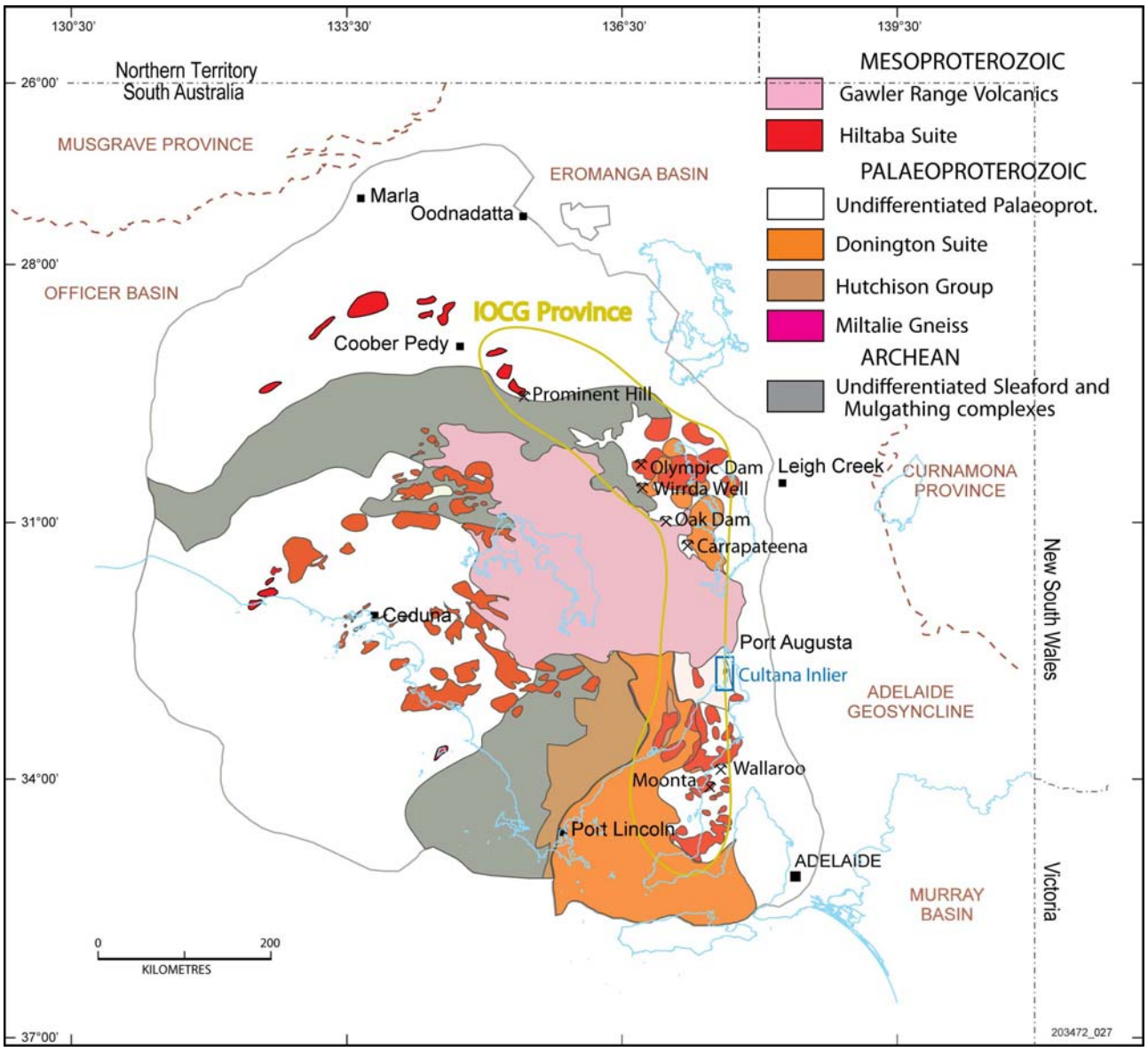

Figure 1. Simplified basement geology map of the Gawler Craton, showing the extent of the Gawler Range Volcanics and Hiltaba Suite Granites, Olympic Cu-Au-(U) province, and location of the Cultana Inlier. Adapted from Hand et al., 2007.

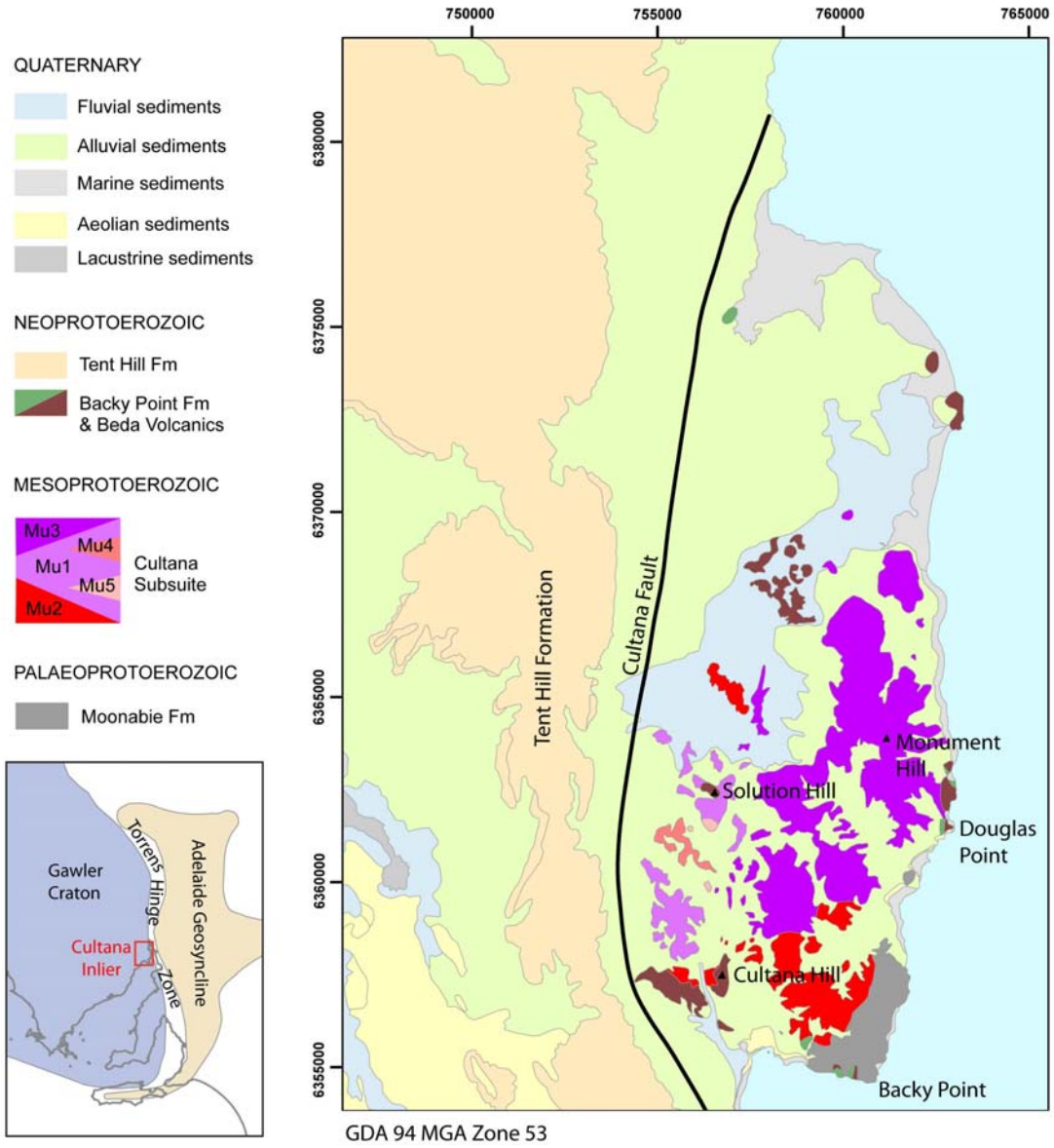

Figure 2. Geology of the Cultana Inlier

DISTRIBUTION AND ACCESS

The Cultana Subsuite is exposed in the Douglas Hills on the north - eastern Eyre Peninsula, extending for up to 7 km from the western coast of the northern Spencer Gulf, between Crag Point and Inshore Hummock (Fig. 3). This irregular group of hills reaches a maximum altitude of 220 m and covers ~50 km^2. The Douglas Hills are located within the Cultana Army Training Area (CATA) (Fig. 3), which is held by the Australian Federal Defence Force, and is used for manoeuvre and firing exercises. Access to this area is restricted, requiring negotiation with the Federal Defence Force. The only exposure of the intrusion outside of the CATA is at Douglas Point, on the western coast of the Spencer Gulf, which is readily accessible by travelling towards Fitzgerald Bay from the Lincoln Highway ~10 km north of Whyalla and following the coastal road northwards (Fig. 3).

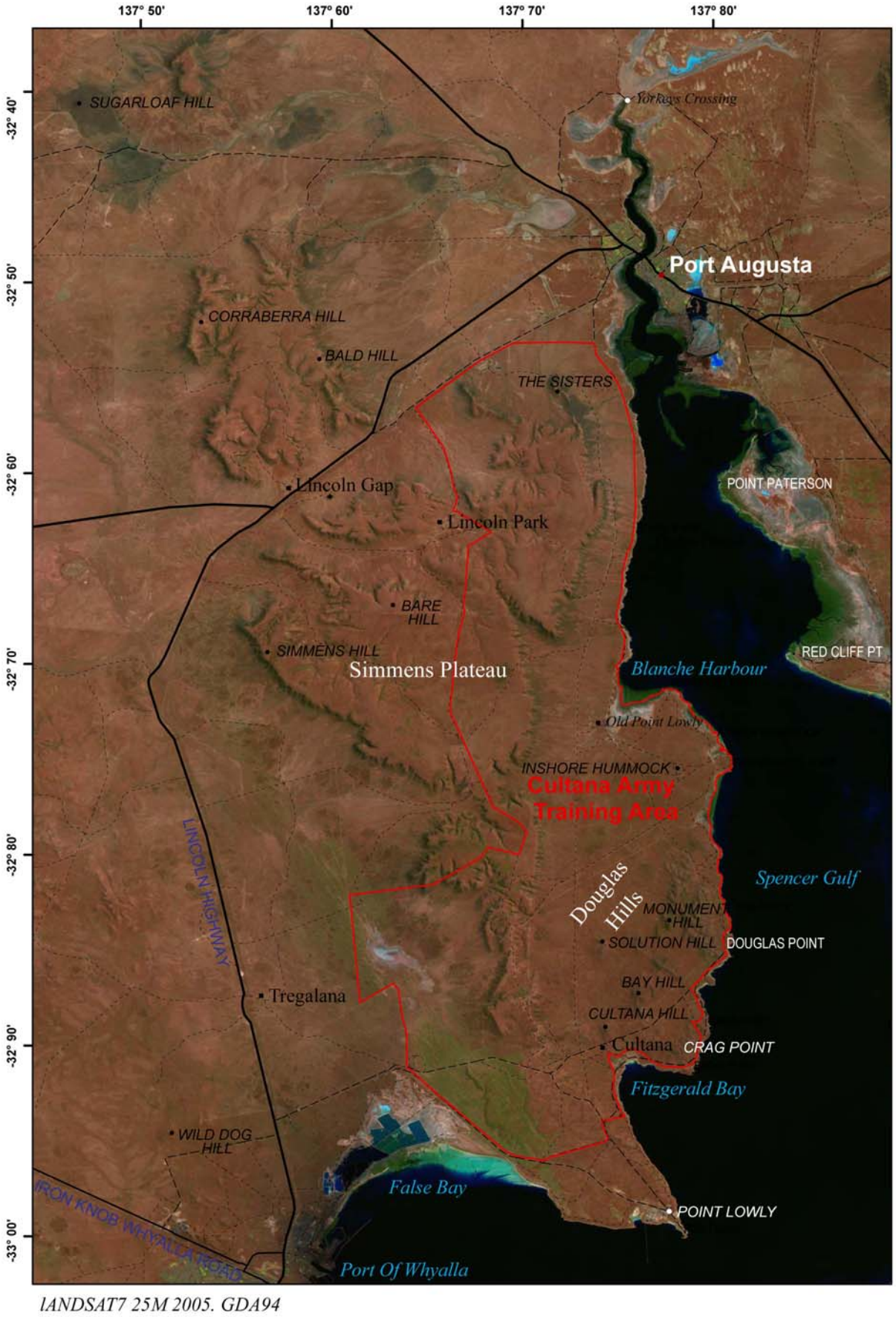

lANDSAT7 25M 2005. GDA94

Figure 3. Topography of the Douglas Hills and surrounds

GEOLOGICAL SETTING

The Cultana Subsuite is exposed within the Cultana Inlier, an uplifted block of Palaeo- to Neoproterozoic rocks bound to the west by the Cultana Fault, which separates the inlier from the flat-lying Neoproterozoic sediments of the Stuart Shelf, the youngest part of the sequence being the Tent Hill Formation, exposed as the Simmens Plateau (Fig. 2). The eastern margin of the craton is flanked by the Torrens Hinge Zone, an area of transitional deformation containing mildly-deformed Neoproterozoic sediments and crystalline basement which separates the folded sequence of Neoproterozoic sediments in the Adelaide Geosyncline from the equivalent flat-lying sequence in the Stuart Shelf (Parker et al., 1993).

The Cultana Subsuite intrudes the Moonabie Formation, a poorly bedded volcaniclastic gritty sandstone which at its type locality west of the Moonabie Range (~45 km SW of Whyalla) overlies and intertongues with the McGregor Volcanics, a suite of bimodal acidic and lesser mafic volcanics (Parker et al., 1988) which were extruded at ~1740 Ma (Fanning et al., 1988). The formation becomes more mature towards the north east, where in the Cultana Inlier it is a massive, heavy mineral banded feldspathic quartzite (Parker et al., 1993). The Moonabie Formation underwent greenschist-amphibolite faces metamorphism and was deformed by NE–SW trending open folds (Parker et al., 1988; Parker et al., 1993) during the Kimban Orogeny (1690–1730 Ma) (Fanning et al., 2007). In the Cultana Inlier the Moonabie Formation has also been locally affected by contact metamorphism during intrusion of the Cultana Subsuite near Crag Point trig (Crawford and Forbes, 1969).

The Cultana Subsuite is unconformably overlain by the Backy Point Formation, a fluvial sandstone which is interlayered with the Beda Volcanics, a sequence of basalt flows which are believed to be the extrusive equivalent of the Gairdner Dolerite (Cowley, 1991). The unconformity can be observed at Douglas Point, and Cultana and Solution Hills. Although not visible in outcrop, the northern part of the Cultana Subsuite is intruded by a swarm of the Gairdner Dolerite dykes (~825 Ma) (Wingate et al., 1998) which are evident in magnetic imagery (see below in Geophysical Signature of the Cultana Inlier).

PREVIOUS STUDIES

There have been few previous studies of the Cultana Subsuite. In their description of the geology of the Cultana 1:63 360 map sheet Crawford et al. (Crawford and Hiern et al., 1964; Crawford and Forbes, 1969) described the felsic intrusive as the ‘Cultana Granite’. The authors reported that they did not examine the Cultana Granite in detail, but that much variation existed within the rocks of the inlier. They observed the existence of porphyritic, granitic and fine grained phases, but did not distinguish these in their mapping. In his 1:500 000 map of the Gawler Ranges, Blissett (1987) differentiated the porphyritic phases of the intrusion as a porphyritic dacite, rhyodacite and rhyolite equivalent to the Gawler Range Volcanics and the granite phases in the north-west of the inlier as equivalent to the Hiltaba Suite. Additional observations have been made of the rocks by exploration companies working in the area, including 1:40 000 scale lithological, geomorphological and structural mapping along the eastern side of the inlier by Craton Resources (2001) and lithological descriptions by Merritt Mining (Fairclough and Cowden, 1998).

DERIVATION OF NAME

The name Cultana is derived from the disused Cultana Homestead (756630 mE 6356300 mN, GDA 94, Zone 53) which is now located within the Cultana Army Training Area. The rocks here defined as the Cultana Subsuite were first referred to in publication as the Cultana Granite by Crawford and Hiern on the Cultana 1:63 360 map sheet (1964) and in the accompanying report (Crawford and Forbes, 1969) . This terminology was followed by a number of other authors (Harding, 1969; Parkin, 1969; Thomson, 1969; South Australia Department of Mines, 1972; Webb et al., 1986; Budd, 1997), but the intrusive has since been referred to in the literature by a variety of other informal names, including the Cultana Granitic Complex (Dalgarno et al., 1968; Sibenaler, 1972; Forbes and Richards, 1975; Olliver and Nichol, 1978), Cultana Granophyre (Thomson et al.,

1976; Anderson, 1980; Budd, 1997), Cultana Granite Complex (Olliver and Nichol, 1978), and Cultana Complex (Geological Survey of South Australia, 1983).

The term Cultana Subsuite (Map Symbol Mu) has been chosen as the formal name of the intrusion for a number of reasons:

- no lithologies within the Cultana Inlier appear to be extrusive, and therefore the formation is considered to be a subsuite of the Hiltaba Suite, and not equivalent to the Gawler Range Volcanics
- a lithological-based name does not adequately describe the diversity of lithologies within the formation, and the term subsuite gives these constituent lithologies equal status
- the term complex was not thought suitable, as the constituent lithologies are mappable and appear to represent textural variations of a single intrusion, rather than complex contacts between multiple pulses of magmatism.

TYPE LOCALITY

The exposure of the Cultana Subsuite at Douglas Point (Fig. 3) has been selected as the type locality, as it lies outside of the CATA, and is thus readily accessible. It can be reached by travelling towards Fitzgerald Bay from the Lincoln Highway ~10 km north of Whyalla, and following the coastal road northwards to Douglas Point (762519 mE 6361100 mN, GDA 94, Zone 53).

The exposure at Douglas Point is representative of the quartz – feldspar porphyry (Mu1, see below for subunits), which is here intruded by quartz, quartz – haematite and tourmaline - feldspar veining and is unconformably overlain by the Backy Point Formation. A number of reference localities representative of the other lithologies within the Cultana Subsuite have been selected, since they are not exposed at the type locality. The reference locality for the alkali feldspar granite (Mu2) is located at Cultana Hill, and the reference locality for the feldspar-phyric granophyric monzogranite (Mu3) alkali feldspar microgranite (Mu4) and micro-syenogranite (Mu5) at Solution Hill.

GEOCHRONOLOGY

A sample of the quartz feldspar porphyry subunit (see below) of the Cultana Subsuite collected ~1 km north of Douglas Point was dated by IDTIMS (Isotope Dilution Thermal Ionisation Mass Spectrometry) by Fanning (1990). Nine grains were analysed, of which eight cluster within error of each other and concordia, and give a weighted mean of the $^{207}Pb/^{206}Pb$ model ages of 1584 ± 3 Ma. These grains are euhedral and most contain simple zoning, suggesting that they are igneous in origin, and that the age represents the crystallisation age of the porphyry. One grain yielded a $^{207}Pb/^{206}Pb$ age of c. 1675 Ma. This grain is optically indistinguishable from the younger grains, and may be inherited from older crustal material (Fanning, 1990).

LITHOLOGIES OF THE CULTANA SUBSUITE

The lithologies of the Cultana Subsuite (Mu) have been differentiated primarily on the basis of texture with a particular focus on phenocryst proportion and composition and groundmass grain size and texture. In some cases the positioning of boundaries has been difficult because of the gradational contacts between the lithologies. Due to restrictions in access mapping coverage of the area during this project was not comprehensive, and was concentrated largely on the northern and western parts of the intrusion. Areas which were not visited were interpreted from field observations by previous survey members, rock samples from the area stored at the PIRSA Glenside Core Library, or existing company and department mapping (Crawford and Hiern, 1964; Cowley, 1991). The following descriptions are based on field and petrographic observations by the author along with a petrographic report by Purvis (2008, see App. 2) and petrological descriptions of samples of the subsuite collected by B.P. Thompson in 1972 (Lowder, 1973) and by Australian Selection when exploring to the west of the inlier on EL212 (1977, see App. 3).

Quartz feldspar porphyry (Mu1)

The quartz – feldspar porphyry (Fig. 4) constitutes the bulk of the exposure of the Cultana Subsuite in the east Douglas Hills. It is composed of abundant quartz phenocrysts (up to 6 mm in diameter) which are commonly round and have resorbed or embayed edges, and rounded sericitised feldspar phenocrysts (up to 4 mm in diameter), in a granular groundmass of fine grained quartz and sericitised feldspar, which is locally granophyric. The groundmass contains small phenocrysts of partly oxidised magnetite up to 1.5 mm, and patches of decussate muscovite which may be replacing primary biotite . The quartz – feldspar porphyry contains a number of small (less than 1 m^2) purple – red aphyric microgranite lens or lozenge shaped bodies of fine grained granular quartz and feldspar. The contact between the porphyry and these bodies is gradational, and likely represents igneous layering.

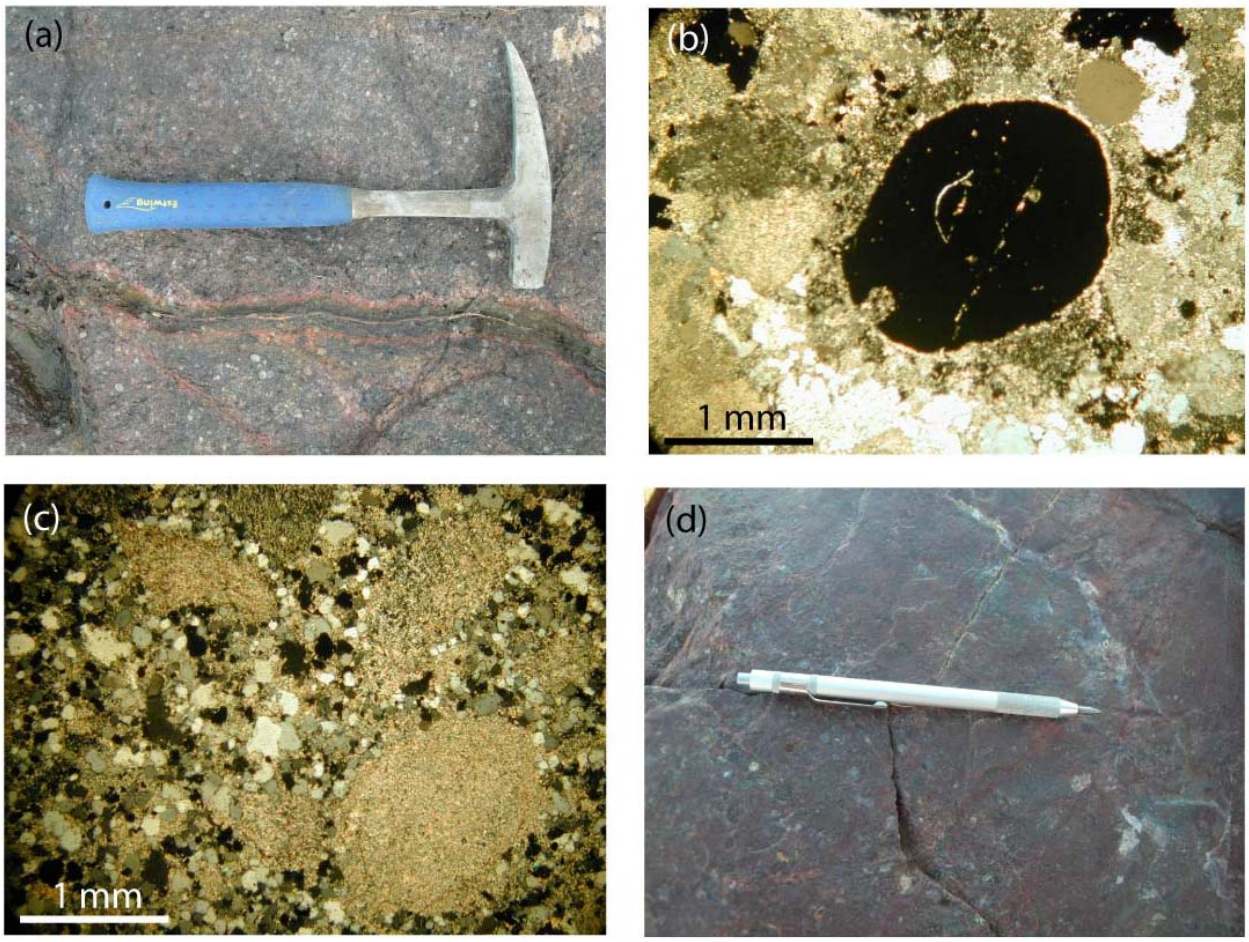

Figure 4. **Quartz - Feldspar Porphyry.** (a) Texture of the porphyry at Douglas Point. (b) Photomicrograph of rounded and embayed quartz phenocryst in a granular groundmass of quartz and sericitised feldspar. (c) Photomicrograph of rounded sericitised feldspar phenocrysts in a granular groundmass of quartz and sericitised feldspar. (d) Fine grained granular quartz and feldspar phase within the quartz - feldspar porphyry.

Alkali feldspar granite (Mu2)

The alkali feldspar granite (Fig. 5) is exposed on the north-west and south-west edges of the intrusion. It is very coarse grained, and is composed predominantly of anhedral grains of perthitic alkali feldspar (up to 10 mm in diameter) which is interstitial to less abundant quartz (up to 8 mm), some grains of which are round and have resorption channels filled with alkali feldspar. Minor plagioclase occurs as small interstitial subhedral crystals and as Rapakivi rims to alkali feldspar crystals. The granite contains minor interstitial tourmaline and opaques, trace fluorite and zircon, and minor muscovite and clay which is probably deuteric in origin. At Cultana Hill the granite

contains late stage coarse grained pegmatitic sweats composed of potassium feldspar, quartz and tourmaline.

The granite contains a weakly granophyric porphyritic phase north of Solution Hill. It is composed of round quartz phenocrysts (up to 6 mm in diameter) and less abundant alkali feldspar phenocrysts (up to 8 mm in diameter), in a groundmass dominated by in-equigranular quartz and haematite-stained alkali feldspar. In places the groundmass is granophyric, ranging from quartz poor to quartz rich (up to 2 mm diameter). Minor plagioclase occurs as inclusions in alkali feldspar phenocrysts and as laths up to 2 mm in the groundmass. Oxides and rutile in the groundmass appear to be a combination of primary and secondary origin. Dark greenish brown tourmaline occurs as poikilitic grains up to 4 mm and is probably deuteric or pneumatolytic.

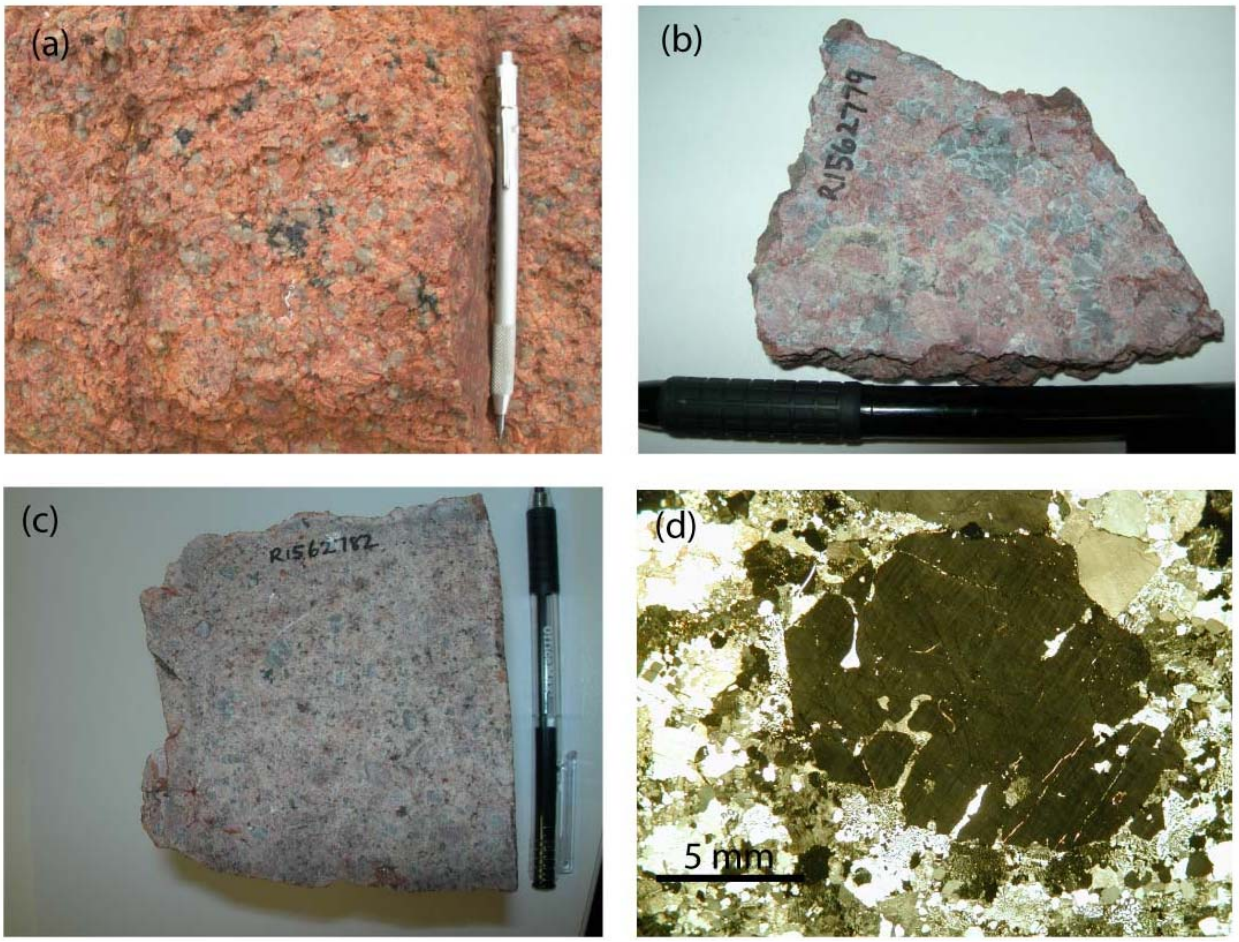

Figure 5. **Alkali feldspar granite.** (a) Rounded quartz and potassium feldspar with interstitial tourmaline. (b) Rapakivi rim to potassium feldspar crystals. (c) Porphyritic granite facies. (d) Photomicrograph of embayed quartz phenocryst surrounded by granophyric quartz and feldspar intergrowth in porphyritic granite facies.

Feldspar-phyric granophyric monzogranite (Mu3)

The feldspar-phyric monzogranite (Fig. 6) is exposed at Solution Hill. It contains large phenocrysts of euhedral to rounded potassium feldspar (up to 10 mm), often rimmed by plagioclase in a Rapakivi texture, plagioclase phenocrysts and lesser round quartz phenocrysts in a granophyric groundmass of quartz and feldspar. Potassium feldspar cores contain kaolinite patches, and plagioclase rims are sericite – haematite altered. Plagioclase phenocrysts are also sericite – haematite altered, highly fritted and contain abundant granophyric patches. The interstitial granophyre is up to 3 mm in grainsize, and contains minor late stage magmatic quartz which is optically continuous with quartz in the adjacent granophyre. The granophyre contains trace zircon, disseminated oxides and widespread haematite ± clay staining. The monzogranite contains a minor microgranite phase on the eastern side of Solution Hill.

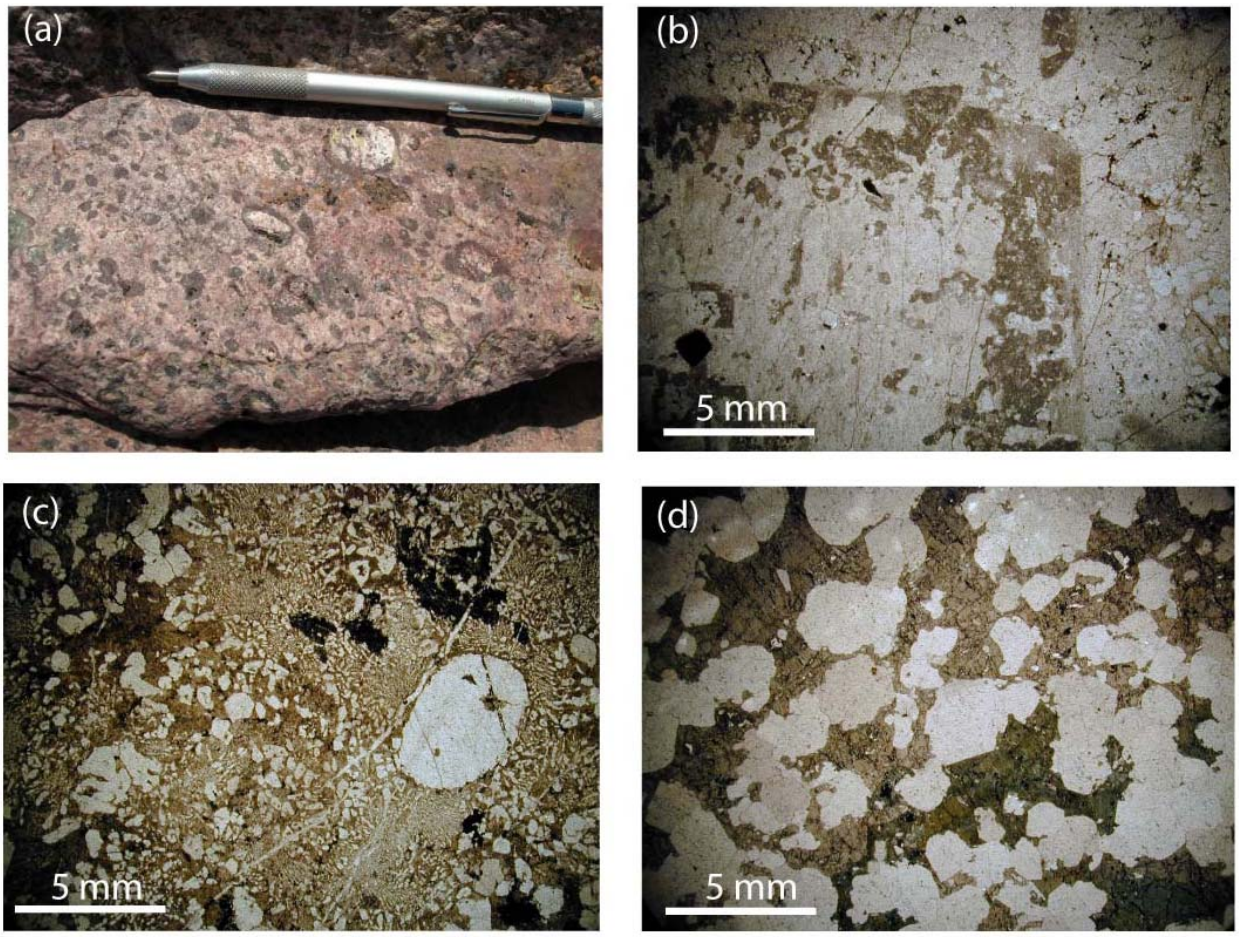

Figure 6. Feldspar phyric granophyric monzogranite. (a) Texture of the monzogranite, composed of altered rounded potassium feldspar phenocrysts with plagioclase rims, and smaller altered feldspar phenocrysts. (b) Sericitised plagioclase rim to potassium feldspar phenocryst. (c) Round quartz phenocryst in granophyric groundmass. (d) Tourmaline - quartz intergrowth in aplitic phase within monzogranite.

Alkali feldspar microgranite (Mu4)

The alkali feldspar microgranite (Figs 7a, b) occurs on the western edge of the intrusion and is poorly exposed. It is pink or pink–purple and is composed of fine grained granular quartz and potassium feldspar (0.1–0.5 mm in diameter) and minor tourmaline. It is weakly porphyritic, containing sparse sericitised anhedral plagioclase phenocrysts (2–10 mm in diameter) and elliptical quartz phenocrysts (up to 3 mm in diameter). It contains small amounts of muscovite, haematite and altered biotite.

Micro-syenogranite (Mu5)

The micro-syenogranite (Figs 7c, d) occurs directly south of Solution Hill, and is only a minor phase within the subsuite. It is composed of a predominantly granophyric, partly granular intergrowth of quartz and alkali feldspar (up to 2 mm in diameter), with lesser altered plagioclase. The plagioclase is altered to sericite and haematite, and minor secondary clay, muscovite and haematite occurs in the groundmass.

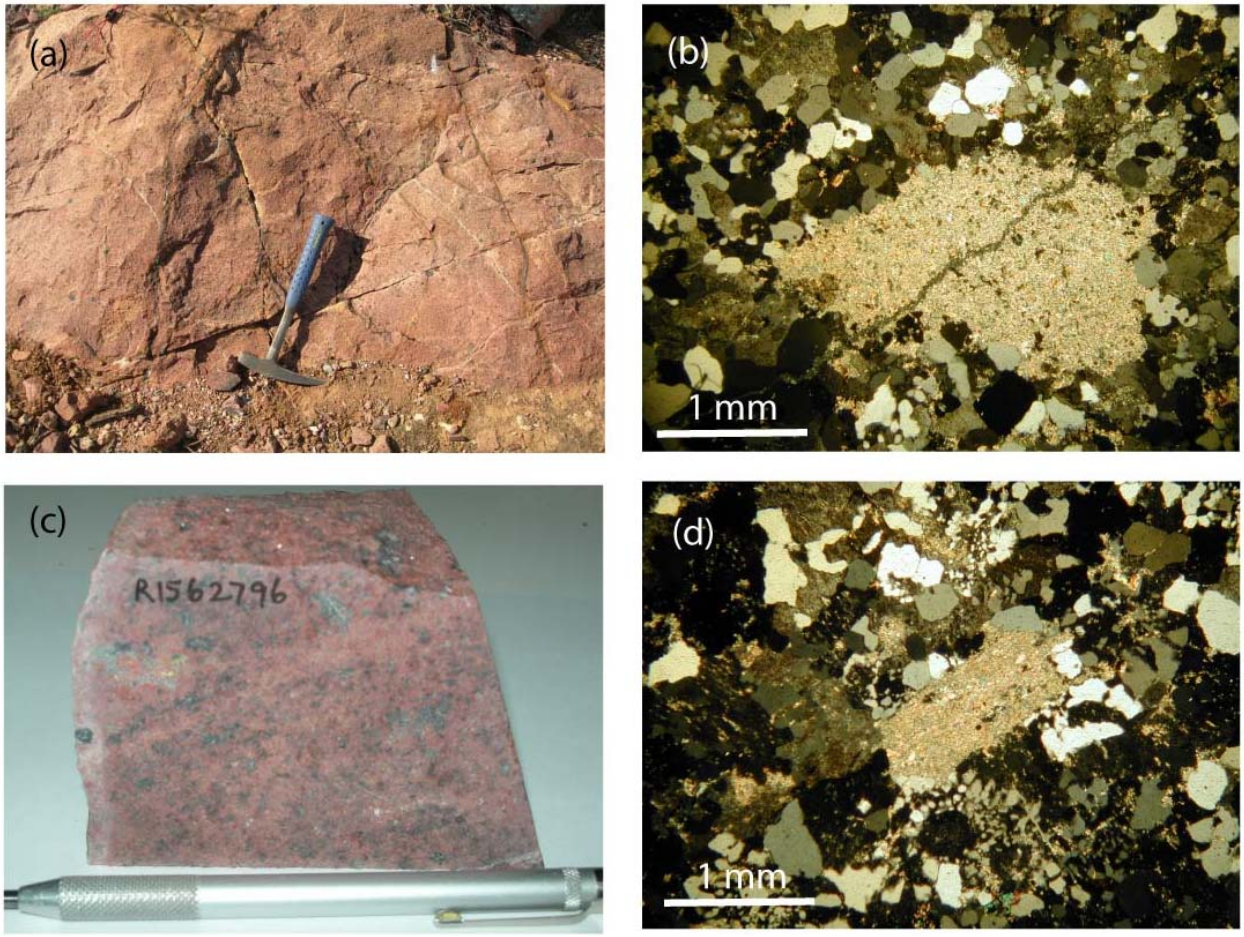

Figure 7. **Microgranite lithologies.** (a) Alkali feldspar micro-granite. (b) Photomicrograph of sericitised feldspar in granular quartz and feldspar groundmass in alkali feldspar micro-granite. (c) Micro-syenogranite. (d) Photomicrograph of sericitised feldspar phenocryst in granophyric groundmass in micro-syenogranite.

PLUTON MORPHOLOGY

The lithologies of the Cultana Subsuite appear to be comagmatic, as no cross-cutting relationships can be observed and the boundaries between the lithologies are transitional, suggesting that the Cultana Subsuite represents a single intrusion. In particular, the feldspar-phyric monzogranite, which is characterised by resorbed phenocrysts in a medium grained granitic groundmass, represents a transitional texture between the alkali feldspar granite (coarse-grained equigranular texture) and the quartz-feldspar porphyry (resorbed phenocrysts in a very fine grained groundmass).

There is a trend in the outcrop pattern of coarser grained lithologies on the western and southern sides of the intrusion and finer grained lithologies on the east (Fig. 2). Alkali feldspar granite is exposed on the northern and southern edges of the intrusion, feldspar-phyric monzogranite on the western edge, and porphyry on the east of the intrusion. The quartz-feldspar porphyry may represent a faster-cooling equivalent of the granites along the eastern edge of the intrusion, which may be a cooling margin of the pluton. Alternatively, the quartz – feldspar porphyry may represent a shallower part of the pluton than the granitic lithologies, the pluton having been tilted by movement on the Cultana Fault.

PHENOCRYST RESORPTION AND RAPAKIVI CHARACTERISTICS

The distinctive mineral textures in the Cultana Subsuite supply information about the physical conditions during emplacement and crystallisation. Many of the quartz and feldspar phenocrysts in the quartz – feldspar porphyry and feldspar-phyric granophyric monzogranite are rounded, indicating that these early crystallising phases have been partially resorbed in the melt (Purvis, 2008). The alkali feldspar granite and feldspar – phyric granophyric monzogranite both contain Rapakivi rims of plagioclase enclosing potassium feldspar phenocrysts. Many mechanisms for the formation of Rapakivi texture have been proposed, including exsolution (Gates, 1953; Hutchison, 1956; Elders, 1966), synneusis (mechanism by which small plagioclase crystals float into growing phenocrysts of potassium feldspar) (Holmquist, 1901; Wahl, 1925; Hibbard, 1979), resorption – infilling (Stull, 1978; Stull, 1979), metasomatic replacement (Hawkes, 1967) and loss of volatiles (Terzaghi, 1940; Stewart, 1956), but the most typical mechanisms are currently considered to be overgrowth by isothermal decompression (Nekvasil, 1991; Eklund and Shebanov, 1999), or magma mixing (von Wolff, 1932; Larsen et al., 1938; Wager et al., 1965; Hibbard, 1981).

Granites with rapakivi texture are commonly associated with comagmatic mafic intrusions (Haapala and Ramo, 1999). The mixing of a cooler felsic magma with a hotter mafic magma brings about quenching of the mafic magma and superheating of the felsic magma. This causes resorption of earlier formed potassium feldspar crystals from the felsic component and rapid crystallisation of plagioclase from the mafic component over potassium feldspar crystals (Hibbard, 1981). Alternatively, at the lower pressure conditions following ascent of the magma the stable feldspar phase shifts from potassium feldspar to plagioclase, and the potassium feldspar is partially resorbed and plagioclase crystallises as rims around potassium feldspar and as phenocrysts (Nekvasil, 1991). There are no mafic phases of the Cultana Subsuite observed in outcrop, although they may potentially be present at depth in the pluton.

Decompression is considered to be the more likely mechanism. There are a number of requirements that must be met for the formation of Rapakivi texture by decompression (Nekvasil, 1991):

- The magma must be sufficiently alkali feldspar - rich to permit saturation or potassium feldspar and plagioclase during the early stages of crystallisation so that the viscosity (degree of crystallinity) remains low enough to allow ascent of the magma.
- The water content of the melt must be low enough at the onset of ascent of crystallisation that it will not become saturated during decompression, which would cause rapid crystallisation.
- The percentage of potassium feldspar crystallising at depth must be high enough that the ascent will not result in its complete resorption.
- Cooling during decompression must be close to adiabatic, or crystallisation rather than resorption would occur.

The presence of a granophyric texture in the feldspar – phyric granophyric monzogranite and micro-syenogranite is the result of rapid simultaneous crystallisation of quartz and feldspar (Barker, 1970) due to undercooling, the lowering of the temperature of the magma below its liquidus temperature (Dunham, 1965). Undercooling of magmas that have ascended close to the surface can be caused by isothermal depressurisation and associated degassing, adiabatic cooling by exsolving expanding vapour or convecting superjacent hydrothermal systems (Lowenstern et al., 1997). The alkali feldspar granite contains miarolitic cavities which indicate late stage volatile saturation, and are common in granites with Rapakivi texture (Nekvasil, 1991).

ALTERATION OF THE CULTANA SUBSUITE

The Cultana Subsuite has been affected by a number of alteration phases with varying degrees of intensity, including sericitisation of feldspar, haematite replacement, tourmaline ± quartz ± feldspar veining, haematite ± quartz veining, microgranite haematite breccia and a haematite – quartz filled

breccia cavity. The alteration is brittle in nature, and some veining has epithermal characteristics, suggesting that it occurred at shallow depth. The older Moonabie Formation and Beda Volcanics and Backy Point Formation overlying the Cultana Subsuite have also been affected by haematite alteration.

Sericitisation

Phenocryst and groundmass feldspar in the Cultana Subsuite has undergone alteration to varying degrees (Fig. 4c). Potassium feldspar and plagioclase are commonly replaced by sericite or sericite – haematite ± quartz. Less commonly, plagioclase is albitised or altered to sericite- albite. Alteration is stronger and more extensive in plagioclase than in potassium feldspar, and is typically stronger in the groundmass feldspar than in the phenocrysts. Alteration is stronger in the porphyry and monzogranite than in the alkali granite, as the former contains more modal plagioclase and is finer grained. Sericitisation of plagioclase is geochemically reflected by a strong depletion of Ca and Na from the subsuite to lower than expected values for the modal proportion of plagioclase present in the rocks, and relative to other Hiltaba Suite granitoids (Fig. 8). Typically the alteration is weak enough to allow identification of the feldspar, but in some samples the alteration in the groundmass is so extensive that its primary mineralogy and texture is completely destroyed.

Haematisation

The Cultana Subsuite has undergone varying degrees of haematite alteration, including haematite staining of potassium feldspar, haematite and sericite replacing feldspar (Fig. 9a), and pervasive haematite replacement of the groundmass (Fig. 9b). Some samples contain up to 39% haematite.

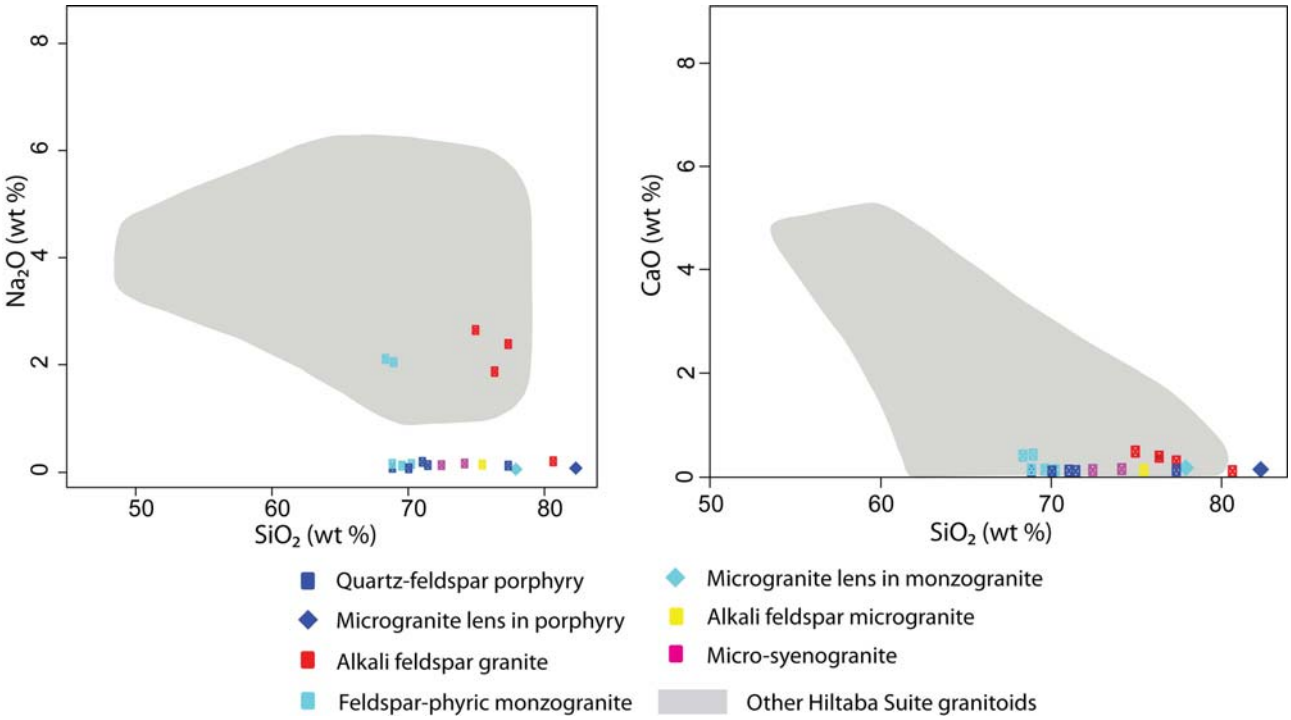

Figure 8. Na_2O (wt %) and CaO (wt %) vs. SiO_2 plots for the Cultana Subsuite overlaid on the data range for other granitoids of the Hiltaba Suite from the Cleve, Coulta, Olympic, Spencer, Wilgena, Nuyts and Moonta Domains, compiled from Stewart and Foden, (2003), Budd, (2006), Creaser, (1989) and Giles, (1980).

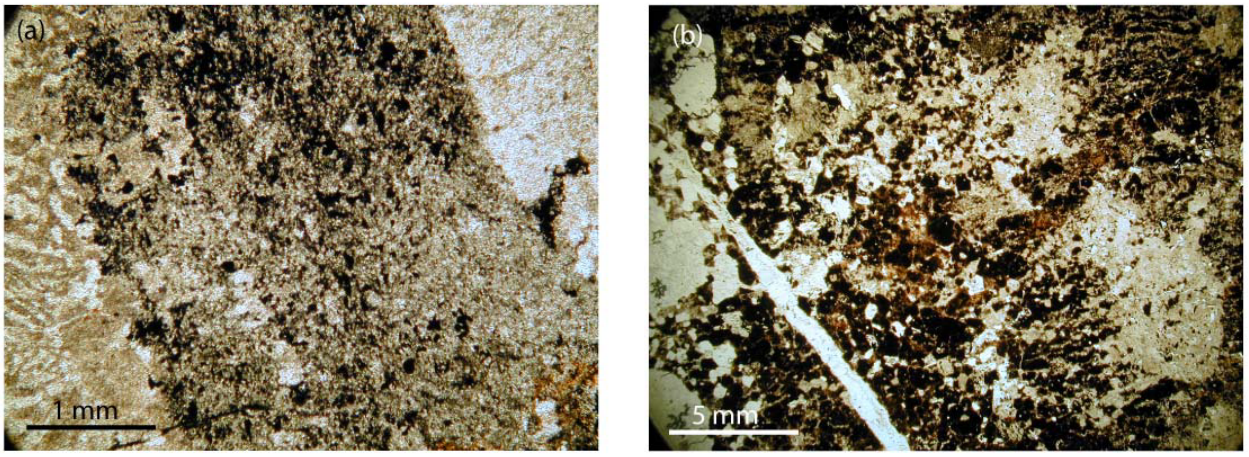

Figure 9. Haematisation of the Cultana Subsuite. (a) Haematite and sericite replacing feldspar in the feldspar phyric monzogranite. (b) Haematite replacement of the groundmass in the quartz feldspar porphyry.

Tourmaline ± quartz ± feldspar veining

Tourmaline is an ubiquitous component in the Cultana Subsuite. As well as being a late stage primary mineral in the alkali feldspar granite and micro-granites, tourmaline also occurs as a secondary veining mineral in all lithologies. It commonly intrudes along fracture planes, from which it invades the groundmass of the rock (Fig. 10a, b), which are often infilled by later quartz veining (Fig. 10c). Tourmaline occurs in larger veins with quartz, as acicular needles radiating from a central point (Fig. 10d). Tourmaline also occurs as thin veins haloed by feldspar (Fig. 10e), and in veins with red haematite – dusted potassium feldspar extending from tourmaline – lined fractures (Fig. 10f).

Haematite ± quartz veining

Haematite ± quartz veining occurs in the quartz-feldspar porphyry and feldspar - phyric monzogranite. The intensity of haematite alteration was observed to be greatest in two locations in the quartz feldspar porphyry, at Douglas Point and in the vicinity of Bay Hill.

At Douglas Point, haematite-quartz veins occur as linear bodies cross-cutting the quartz-feldspar porphyry, predominantly striking N–S and SSW–NNE and steeply dipping. The veins are typically in the order of 20–40 mm thick and are occasionally zoned with earlier haematite forming the outer part of the vein and later quartz filling the central part of the vein (Fig. 11a, b). The haematite is blue–grey and has a fibrous or tabular habit, with the plates often orientated with their broad side orthogonal to the vein edge. The quartz ranges in composition from clear to amethyst, and is often perfectly euhedral in form.

Intense haematite veining occurs in the vicinity of Bay Hill in close proximity to the micro-granite haematite breccia (described below). Thin haematite veins typically 1–3 mm thick intrude the quartz feldspar porphyry in many orientations but predominantly N–S and E–W (Fig. 11c). The haematite occurs in two phases, blue–grey haematite veins with sharp contacts, and red haematite typically flanking the blue haematite veins which has pervaded the groundmass of the porphyry (Fig. 11d).

Figure 10. Tourmaline veining. (a) Tourmaline lining fractures in feldspar phyric monzogranite. (b) Tourmaline veins and blebs in alkali feldspar micro-granite. (c) Tourmaline permeating groundmass along fracture in feldspar phyric monzogranite, with later quartz infill. (d) Tourmaline – quartz vein. (e) Tourmaline veins with feldspar 'halo'. (f) Tourmaline and haematite-dusted feldspar vein at Douglas Point.

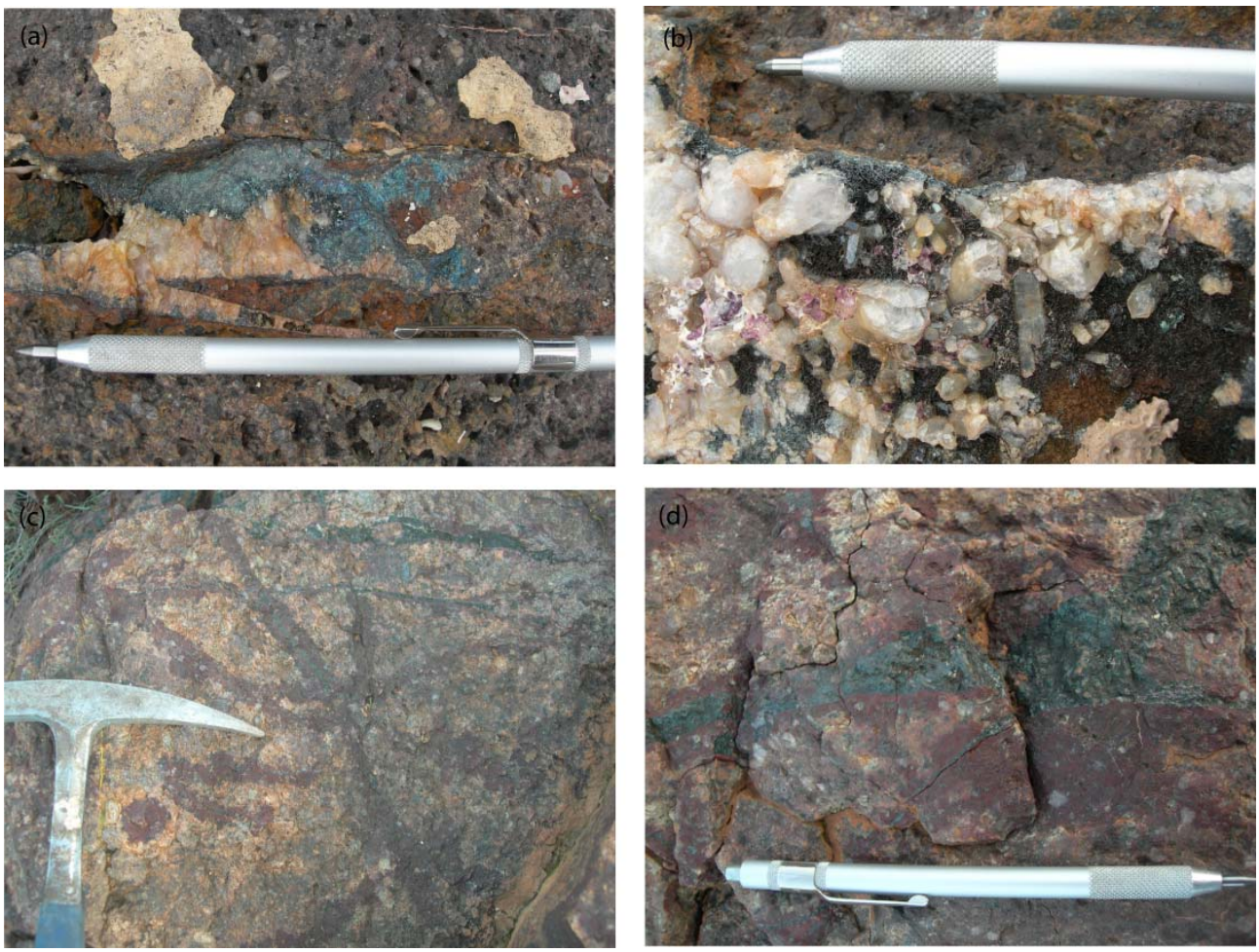

Figure 11. Haematite – quartz (a-b) and haematite stockwork veining (c-d) in the Cultana Subsuite. (a) Haematite – quartz vein intruding the quartz feldspar porphyry. (b) Detail of haematite – quartz vein with acicular haematite and euhedral clear to amethyst quartz. (c) Stockwork haematite veining. (d) Detail of stockwork haematite vein with phases of blue and red haematite.

Monomict micro-granite haematite breccia

A breccia body occurs within the haematite – veined quartz feldspar porphyry near Bay Hill (see above). The breccia body occurs as an isolated exposure ~10 m^3 surrounded by porphyry outcrop, but the contact between these two rocks is not observed. The breccia contains a single population of angular to subrounded pink–orange clasts of quartz – sericite rock ranging in size from 1–20 cm in a fine grained haematite – rich matrix (Fig. 12a). The breccia has a clast to matrix ratio of ~4:1, and the matrix occurs in thicknesses up to 5 cm. There are sections of the breccia which are clast dominant (~95%) and composed of angular clasts in a 'jig-saw' texture separated by only a thin (<1 mm) matrix. These clasts appear to have been fractured and cemented in situ without rotation or transportation. The sections of 'jig-saw' breccia are typically 4–15 cm in diameter, and may be clasts of an earlier brecciation event.

The clasts are composed of a fine grained quartz - sericite rock which has no preserved igneous texture (Fig. 12b), but most likely represents an altered micro-granite or aplite which has been transported along the breccia zone, or a late intrusive plug within the porphyry which has been the focus of brecciation. The clasts are commonly sericitised around their edges and contain haematite veining, and the groundmass of the clasts has been invaded by haematite (Fig. 12c–d).

The breccia is most likely to be hydrothermal in origin. Mechanical energy is released from a hydrous magma in a subvolcanic environment during second boiling and subsequent decompression (Burnham, 1985). During second boiling a water saturated melt is converted to a mix of crystals and water vapour, which is associated with an increase in volume which creates

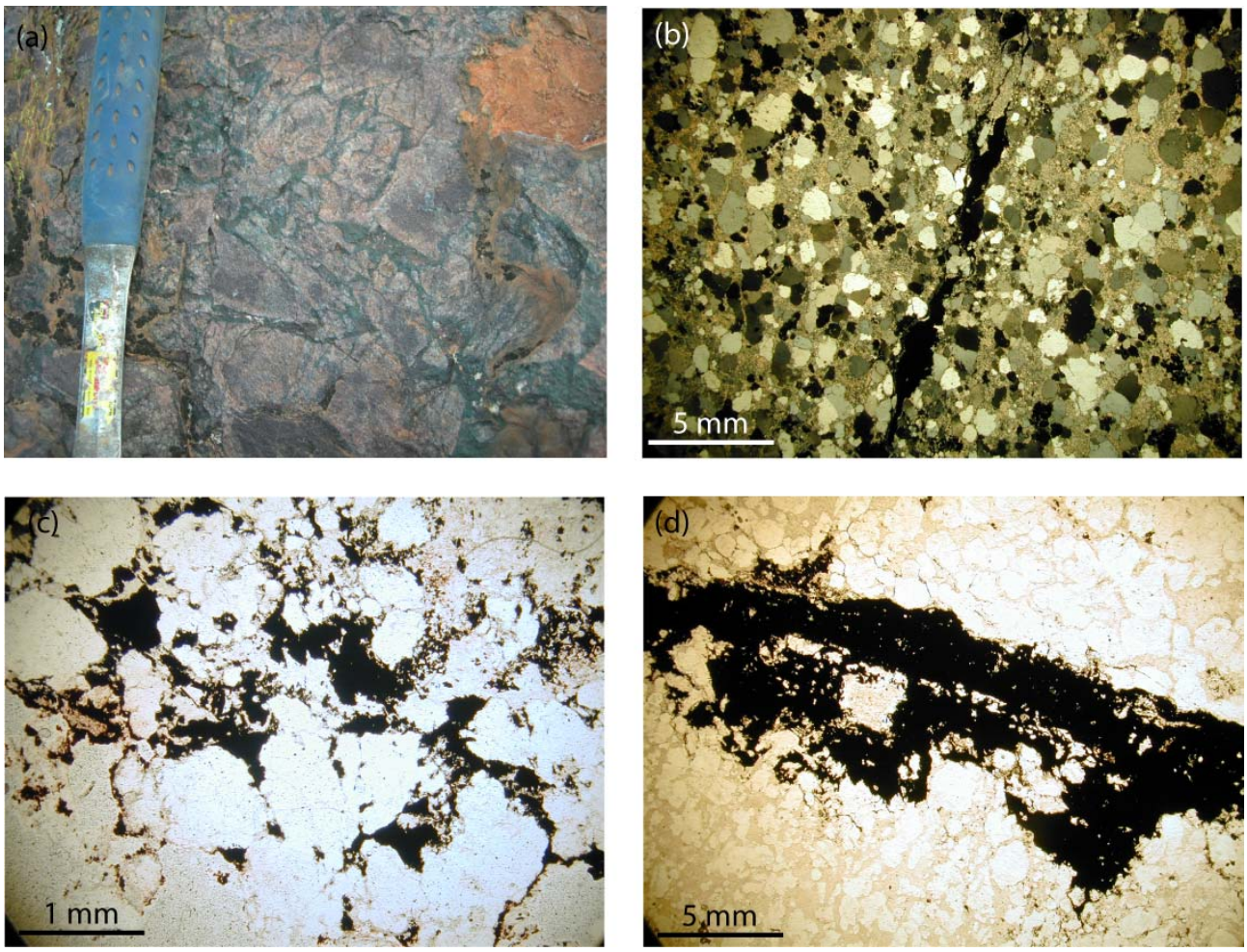

Figure 12. Haematite breccia in the quartz feldspar porphyry. (a) Aplitic haematised clasts with sericitised margins in a haematite rich matrix. (b) Photomicrograph of quartz – sericite clast. (c) Haematite replacement of sericite between quartz grains. (d) Haematite matrix between clasts, containing clast fragments.

sufficient energy to fracture wall rocks to depths of 4–5 km. Decompression of water-saturated melt and previously exsolved aqueous fluid leads to an expansion of exsolved water into the fracture system, and releases further energy (Burnham, 1985).

Haematite – quartz-filled breccia cavity

A haematite – quartz filled breccia cavity occurs within the quartz feldspar porphyry in close proximity to the breccia described above (Fig. 13a). The cavity is ~30 cm thick and 60 cm long and has been filled by two successive fluid phases now represented by two compositional zones, a peripheral siliceous zone and an inner haematite zone. The siliceous zone is found in the bottom and eastern edge of the cavity and contains angular clasts of porphyry ranging in size from 2–5 mm in a white silica matrix (Fig. 13b). The top and western edge of the cavity is lined by a rim of aligned euhedral quartz crystals. The haematite zone contains clasts of quartz – feldspar porphyry ranging in diameter from 20–60 mm, typically with a complex morphology and concave faces (Fig. 13c). The clasts are rimmed by aligned euhedral quartz crystals and are largely aggregated in the centre of the pod, and sit in a haematite matrix.

Cavities can be created in a pluton in a number of ways, such as the localised dissolution of rock by fluids, the explosive release of volatiles, or the development of a bubble on the roof of the intrusion (Burnham, 1985), and due to its close proximity is likely to be associated with the same hydrothermal episode which generated the microgranite breccia described above. A likely genesis for the cavity and infill is that the clasts of the porphyry were fractured by fluids which travelled

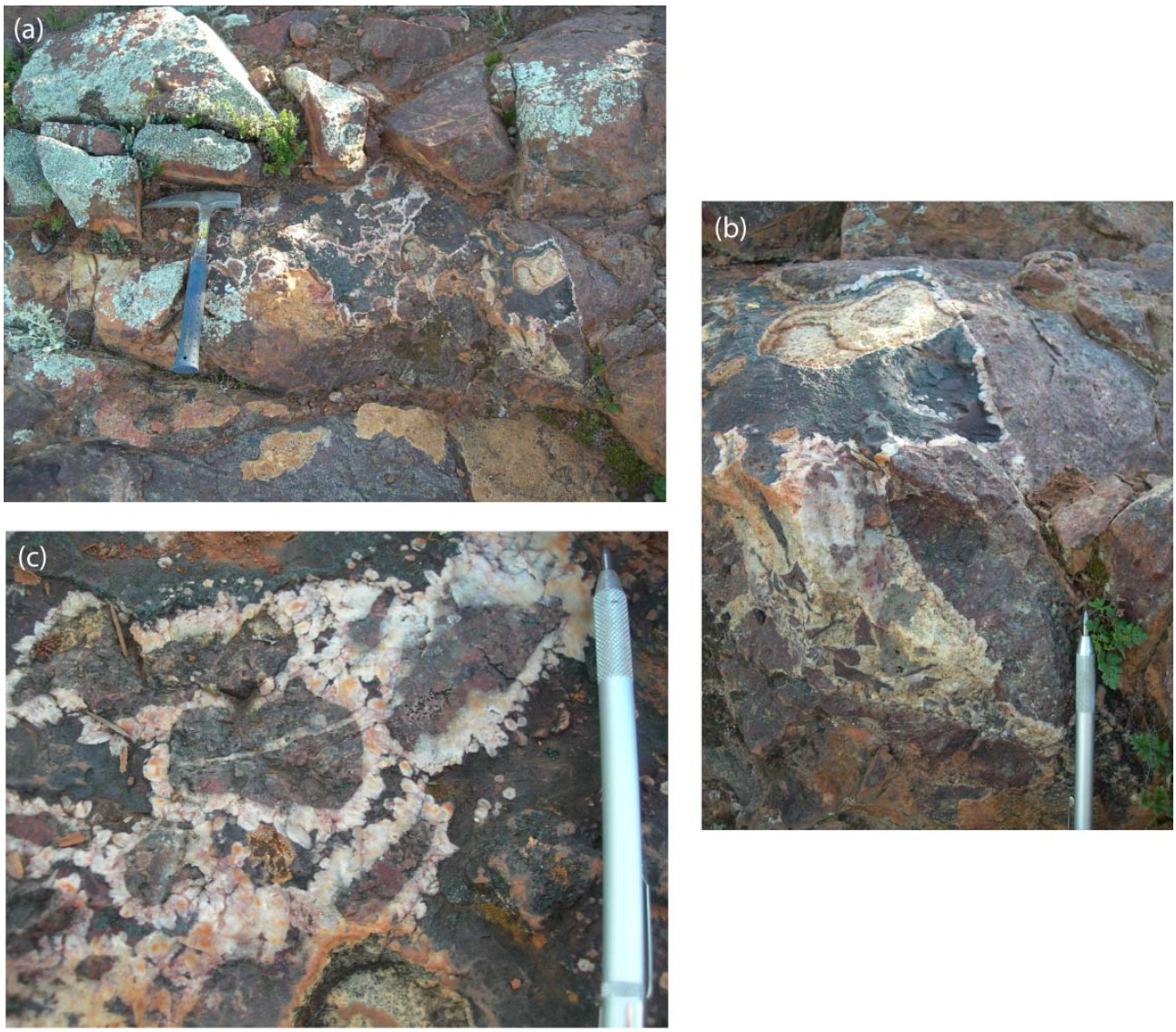

Figure 13. Haematite – quartz filled cavity. (a) Cavity outcrop. (b) Small angular porphyry clasts in a silica matrix. (c) Large porphyry clasts rimmed with quartz in a haematite – rich matrix.

through the cavity. Quartz was the first crystallising phase, forming the siliceous zone and rim to the cavity, and precipitated around clasts while they were suspended in the fluid. Haematite was the late crystallising phase, and formed the matrix of the breccia.

Haematite alteration in the Moonabie Formation

Similarly to the Cultana Subsuite, the Moonabie Formation has been affected by haematite – rich alteration, which is particularly prevalent at Backy Point. It contains steeply dipping haematite veins orientated principally NNE – SSW and a lesser population ESE – WNW, and permeating the bedding plane (Fig. 14a). There are also steeply dipping NNE – SSW breccia zones, composed of Moonabie Formation and quartz clasts in a haematite matrix (Fig. 14b–c), and quartz veins containing haematite clasts (Fig. 14d). The Moonabie Formation also contains minor tourmaline – quartz veining.

Figure 14. Haematite alteration in the Moonabie Formation. (a) N – S, E – W and subhorizontal haematite veining, looking N. (b) N – S striking breccia with haematite rich matrix, looking E. (c) Haematite breccia, looking E. (d) Vein with haematite fragments in a quartz matrix, looking E.

Haematite alteration in the Beda Volcanics and Backy Point Formation

The Willouran Beda Volcanics and Backy Point Formation have also been affected by localised haematite alteration. At Backy Point the Beda Volcanics and the Backy Point Formation have been strongly haematised (Fig. 15). These formations also contain minor tourmaline – quartz veining typically orientated N–S.

The occurrence of clasts of Cultana Subsuite lithologies and haematite - quartz and tourmaline-quartz rock in a conglomeratic horizon of the Backy Point Formation at Solution Hill, which unconformably overlies the feldspar – phyric monzogranite indicates that the haematite alteration and tourmaline veining observed in the Cultana Subsuite event occurred before the Willouran, and that a later alteration episode of similar mineralogy also occurred after this time, affecting the Beda Volcanics and Backy Point Formation.

Figure 15. Haematised sandstone of the Backy Point Formation

Fracture and vein system

The vein – hosted alteration in the Cultana Subsuite has a dominant steeply dipping N–S striking orientation (Fig. 16a), and has utilised a fracture/joint system which is steeply dipping and strikes N–S and E–W. The haematite veining and brecciation in the underlying Moonabie Formation shares a similar orientation, striking NNE–SSW and steeply dipping, with a smaller moderately SE – dipping population which has intruded along the bedding plane (Fig. 16b). The fact that the principal fracture and veining set observed in the Cultana Subsuite is also observed in the Moonabie Formation suggests that it is not attributable to contraction during crystallisation of the magma body, but is tectonic in origin, and implies a least principal stress (σ_3) orientated E–W to ESE–WNW.

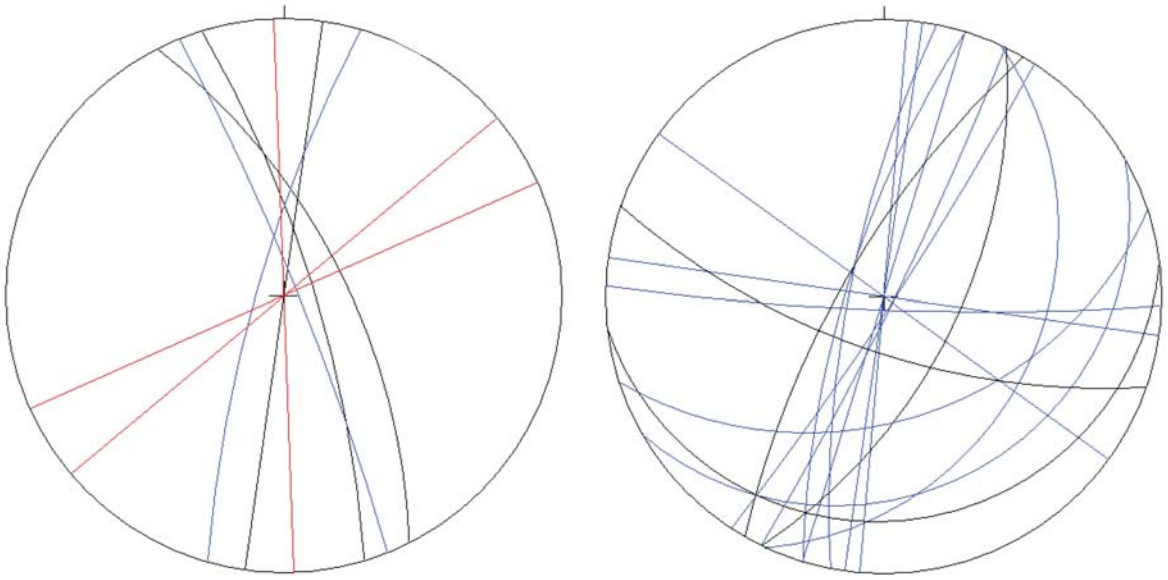

Figure 16. Equal area stereographic projections of planar structures in (a) Cultana Subsuite (N=9) and (b) Moonabie Formation (N=21). Blue represents haematite ± quartz veining, black represents quartz veining and red represents tourmaline ± quartz ± feldspar veining. Plotted using GEOrient © 9.2.

Alteration zoning

There is a distinct spatial distribution to the replacement, veining and brecciation in the Cultana Inlier described above (Fig. 17). Of the Cultana Subsuite, the alkali feldspar granite has been affected by the weakest alteration, containing weak sericitisation of feldspars and tourmaline ± quartz veining. The quartz – feldspar porphyry, feldspar-phyric granophyric monzogranite, alkali feldspar microgranite and micro-syenogranite have been affected by a greater alteration intensity, namely strong sericitisation, moderate haematite replacement, tourmaline ± quartz ± feldspar veining and haematite ± quartz veining. The greatest alteration intensity in the Cultana Subsuite is restricted to a localised area in the vicinity of Bay Hill, where the quartz – feldspar porphyry has been affected by strong sericitisation and haematisation, intense haematite veining, brecciation and the haematite – quartz filled breccia cavity fill. Other as yet undocumented localities of similar high intensity alteration may exist elsewhere within the subsuite. At Backy Point the Moonabie Formation hosts an area of moderate alteration consisting of haematite veining and haematite breccia.

Quartz veining

Quartz-only veining striking predominantly N-S and steeply dipping is observed in the Cultana Subsuite, Moonabie Formation and Backy Point Formation and Beda Volcanics. At Douglas Point quartz veins are observed to be continuous across the unconformity between the quartz – feldspar porphyry and the Backy Point Formation, indicating that at least some of this veining is Neoproterozoic or younger, and not associated with the haematite ± quartz and tourmaline ± quartz ± feldspar veining in the Cultana Subsuite described above.

GEOCHEMISTRY

Twenty two rock samples of the Cultana Subsuite, including representative samples of the different lithologies in the subsuite, and samples affected by varying degrees of alteration, were analysed for a suite of elements at Amdel by a combination of ICP-OES (inductively coupled plasma optical emission spectroscopy), ICP-MS (inductively coupled plasma mass spectroscopy) and fire assay. The sample localities and geochemical results are presented in Appendix 4.

Major elements

There is a distinguishable difference in the major element geochemistry of the porphyritic lithologies (the quartz feldspar porphyry and feldspar phyric monzogranite) compared to the equigranular granitic lithologies (alkali feldspar granite, alkali feldspar microgranite and micro-syenogranite) (Fig. 18). The porphyritic lithologies are typically lower in silica (68.9–77.4 wt %, averaging 70.5 wt %) than the granitic lithologies (75–80.7 wt %, averaging 77.4 wt %), and higher in P_2O_5, Al_2O_3, TiO_2, Fe_2O_3, and MgO. The higher Al_2O_3 and Fe_2O_3 values may be a product of the more pervasive sericite and haematite alteration concentrated in the porphyritic lithologies. CaO and Na_2O values of both porphyritic and granitic lithologies have a bimodal pattern, consisting of a population of low values (averaging 0.10% and 0.13% respectively), which are low for a typical granitic rock and are likely to represent samples in which the feldspars have been pervasively sericitised, and a population of higher values (averaging 0.38% and 2.21% respectively) which are likely to represent samples in which feldspars are only weakly sericitised. K_2O values have a scattered range in both porphyritic and granitic lithologies, which may similarly reflect differential depletion due to sericitisation.

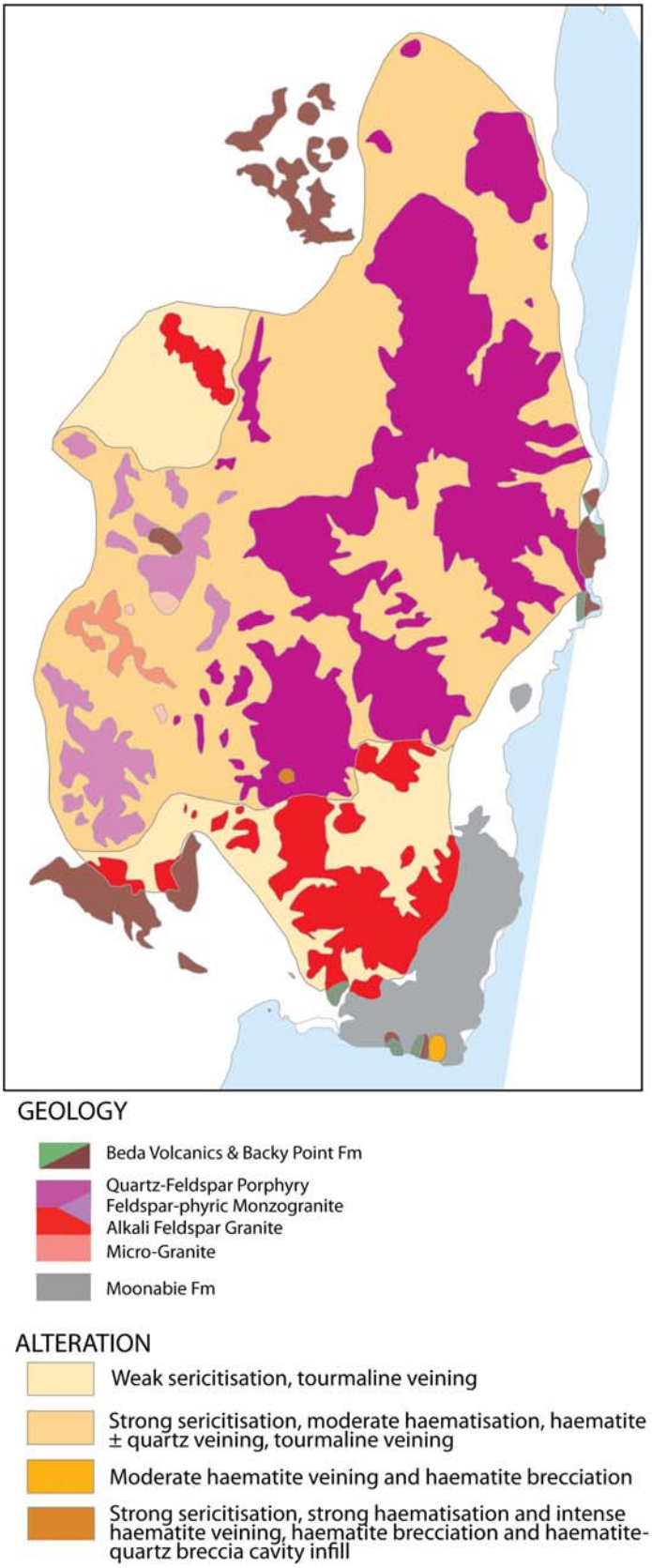

Figure 17. Alteration map of the Cultana Inlier, delineating areas defined by different alteration mineralogies and intensities

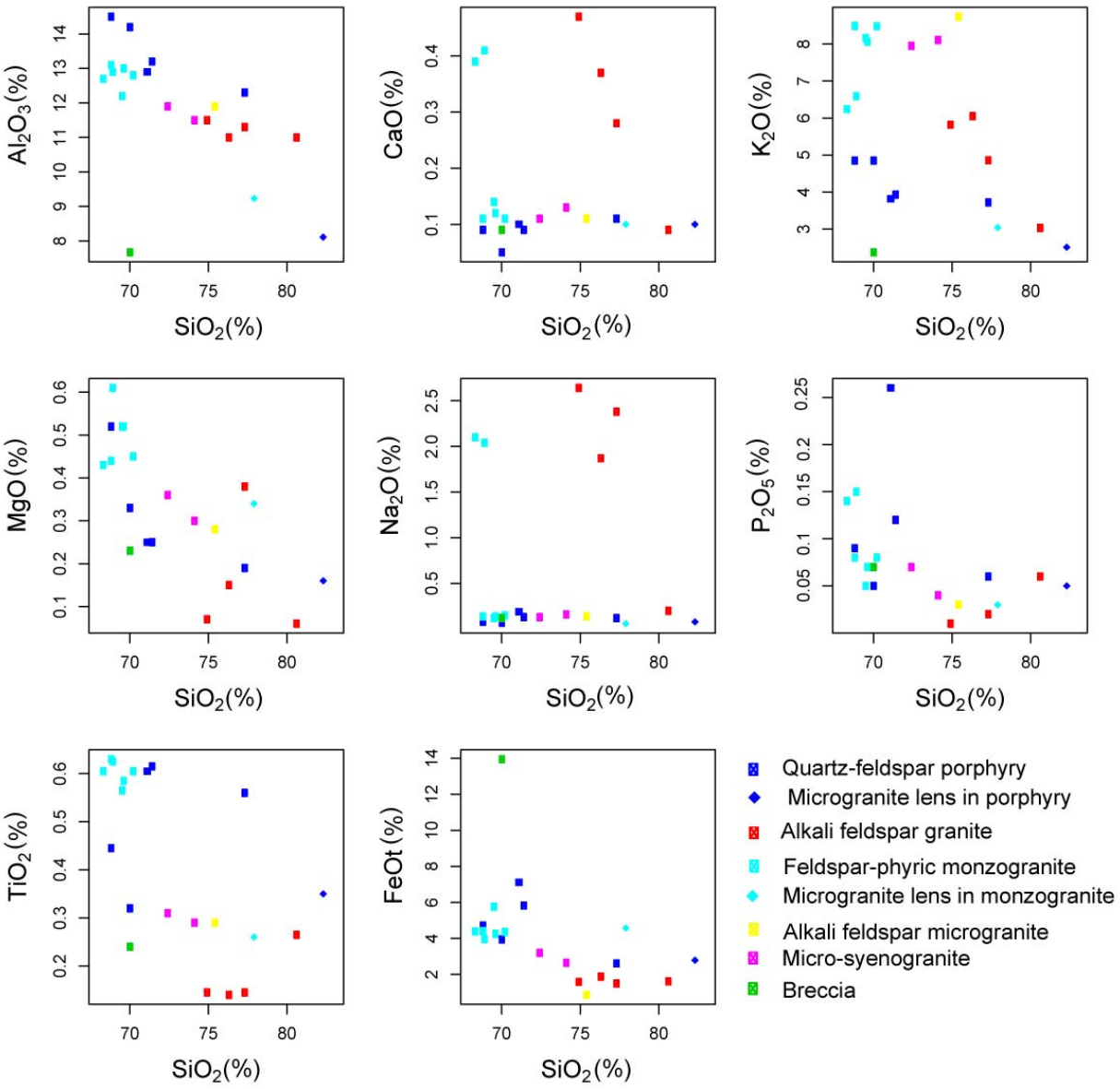

Figure 18. Major oxides (wt %) vs. SiO_2 (wt %) in the Cultana Subsuite

Trace elements

The trace element pattern of the Cultana Subsuite is broadly typical of other Hiltaba Suite granitoids with depletions in Ba, Nb Sr, P and Ti (Fig. 19). However, the Rb depletion is atypical for Hiltaba Suite granitoids, and may be an artefact of the sericitisation of the Cultana Subsuite, because in a granitic melt Rb is strongly partitioned to feldspar (Rollinson, 1993), and being a mobile element may have been removed from the system during alteration.

Similarly to other Hiltaba Suite granitoids, the Cultana Subsuite is enriched in rare earth elements (REE) (Fig. 20). Although REE enrichment can be associated with IOCG – style alteration and mineralisation (Oreskes and Einaudi, 1990; Belperio et al., 2007), the REE levels in the Cultana Subsuite are within the typical range of Hiltaba Suite granitoids (Stewart and Foden, 2003) and variations between lithologies are believed to reflect differences in crystallisation, rather than alteration. The lithologies of the subsuite generally share a similar trend in light REE (LREE), typified by decreasing enrichment with increasing atomic number, and a negative Eu anomaly due to fractional crystallisation of plagioclase (Rollinson, 1993). However, the lithologies of the subsuite have distinctive patterns in the middle and heavy REE (HREE).

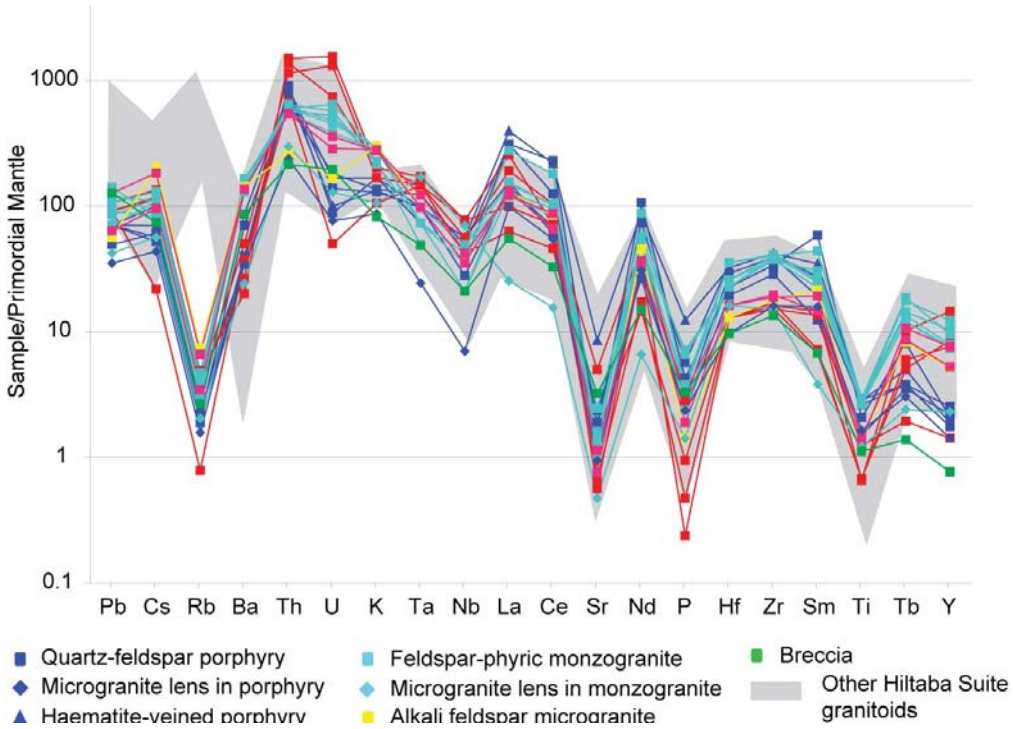

Figure 19. Primordial mantle normalised trace element variation diagram, using normalisation values of McDonough et al., (1992), and P normalisation value of Sun, (1980), quoted in Rollinson, (1993). Data for other Hiltaba Suite granitoids (N=500), including the Cleve, Coulta, Olympic, Spencer, Wilgena, Nuyts and Moonta Domains, is compiled from Stewart and Foden, (2003), Budd, (2006), Creaser, (1989) and Giles, (1980).

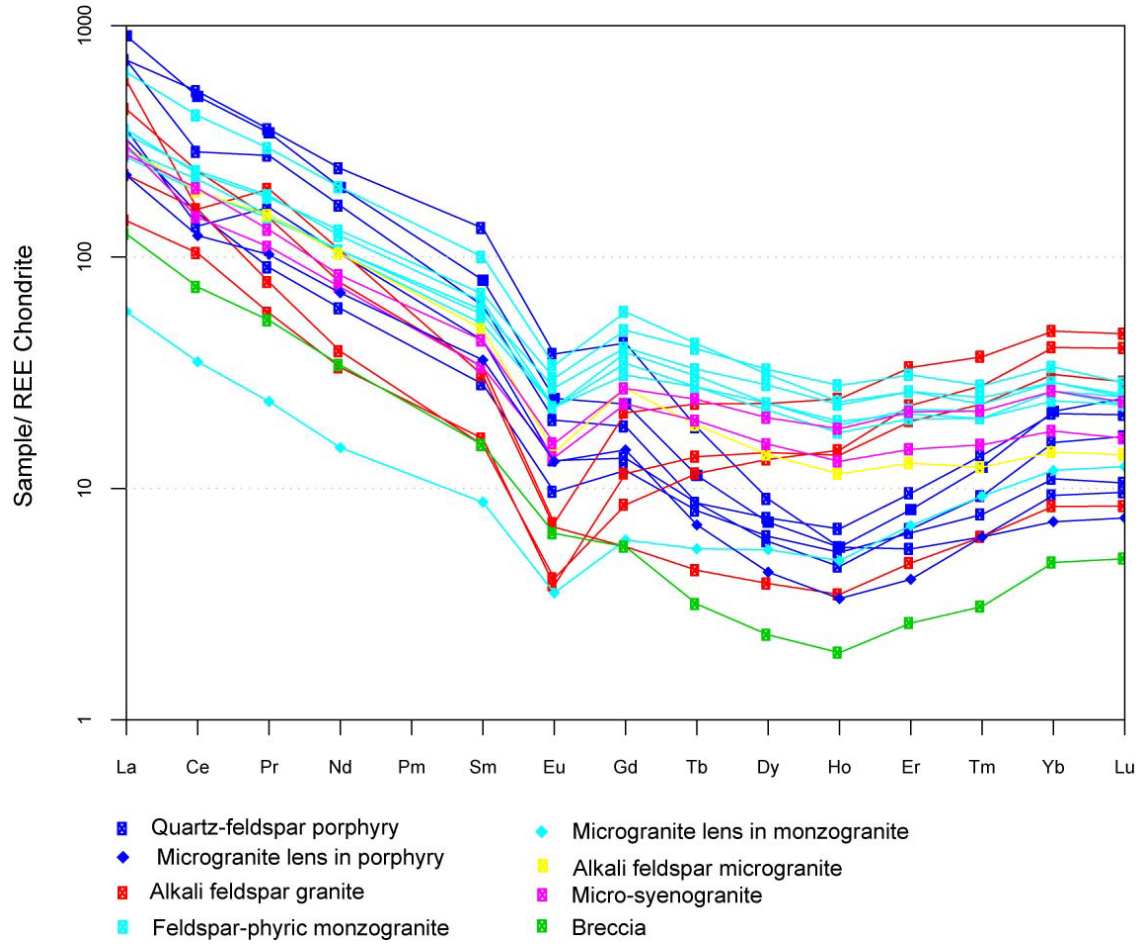

Figure 20. Chondrite normalised REE variation diagram (Bonython, 1984)

The quartz-feldspar porphyry has the greatest enrichment in LREE of the lithologies in the Cultana Subsuite, and has a strong middle REE negative anomaly in Tb, Dy, Ho, Er and Tm (Ho/Gd ratio of 0.31). The microgranite lens and the microgranite haematite breccia in the quartz - feldspar porphyry shares the same trend in REE as the porphyry, but with the lower REE levels.

The feldspar - phyric monzogranite has a similar enrichment in LREE to the quartz-feldspar porphyry, but has a higher enrichment in HREE, which increases with increasing atomic number (Ho/Gd ratio of 0.53). The alkali feldspar microgranite and micro-syenogranite share a similar trend to the feldspar – phyric microgranite, but are slightly lower in REE concentration. The alkali feldspar granite is lower in LREE than the porphyritic lithologies, and has a strong enrichment in HREE increasing with increasing atomic number (Ho/Gd ratio of 1.17).

Granite classification and source of magma

Many geochemical classification schemes of plutonic rocks in popular use rely on alkali elements and iron (i.e. Cox et al., 1979; De la Roche et al., 1980; Debon and Le Fort, 1983; Middlemost, 1985; Frost et al., 2001). Due to the sericite and haematite alteration of the Cultana Subsuite described above, the application of such classification schemes is problematic. The modified alkali lime index (MALI) (Fig. 21a) spreads across the calcic, calc-alkalic, alkali-calcic and alkalic fields, with the least altered samples, based on absence of sericite alteration, being alkali feldspar granites which plot in the alkali-calcic and alkalic fields. All other samples exhibit moderate to strong degrees of sericitisation, with the feldspar-phyric monzogranite and microgranites plotting in the alkalic field and the quartz-feldspar porphyry plotting in the calcic to calc-alkalic field and the minor microgranite phases in the calcic field. The Fe* number of samples is high, with all but two outliers plotting in the ferroan field (Fig. 21b).The data forms two clusters on an ASI (aluminium saturation index) plot (Fig. 21c), with the alkali feldspar granite, feldspar-phyric monzogranite and microgranites plotting between 1–1.4, and the quartz feldspar porphyry and microgranite pods between 2.6–3, all in the peraluminous field.

The replacement of feldspar by sericite commonly occurs by the reaction

$3(K, Na)AlSi_3O_8 + 2H^+ \rightarrow (K, Na)Al_3Si_3O_{10}(OH)_2 + 6SiO_2 + 2(K, Na)^+$.

Where feldspar is replaced volume-for-volume by sericite, such as we typically observe in the feldspar phenocrysts of the Cultana Subsuite, Al must be introduced to the system since sericite has more than twice the Al per unit volume than occurs in the same volume of feldspar, which reaction also involves a loss of alkali elements to solution (Collins, 1997). As a result, the ASI value [Al/(Ca – 1.67P + Na + K)] of a sericitised igneous rock is likely to be greater than the primary igneous value, and the MALI value [$Na_2O + K_2O – CaO$] of a sericitised rock lower than the primary igneous value. The Fe* number [$FeO^{tot}/(FeO^{tot} + MgO)$] is likely to be an overestimate, given that the majority of iron oxide in the samples appears to be secondary.

As a consequence of the alteration of the rocks it is difficult to categorise the chemistry of the subsuite, and suggest the source of the magma from which the pluton is derived. Mineralogically, the presence of tourmaline and lack of amphibole and pyroxene is more consistent with a peraluminous granite derived from crustal melting (Barbarin, 1999). Such granitic rocks typically contain igneous biotite and muscovite, which is rarely observed in the Cultana Subsuite but if present would have likely been replaced by sericite. This is consistent with the depletion in Nb (Fig. 19) which is characteristic of continental crust, and the presence an inherited zircon (c.1675 Ma) in the quartz – feldspar porphyry dated by Fanning (1990) which both suggest a crustally-derived component to the magma (Rollinson, 1993).

The depletion of middle REE in the porphyritic lithologies suggests that the subsuite may have fractionally crystallised from a more mafic magma, as hornblende and sphene, minerals more typical or intermediate to mafic compositions, have high partition coefficients for the middle REE (Rollinson, 1993). Similarly, trace element modelling by Budd (2006) for the Kychering Granite

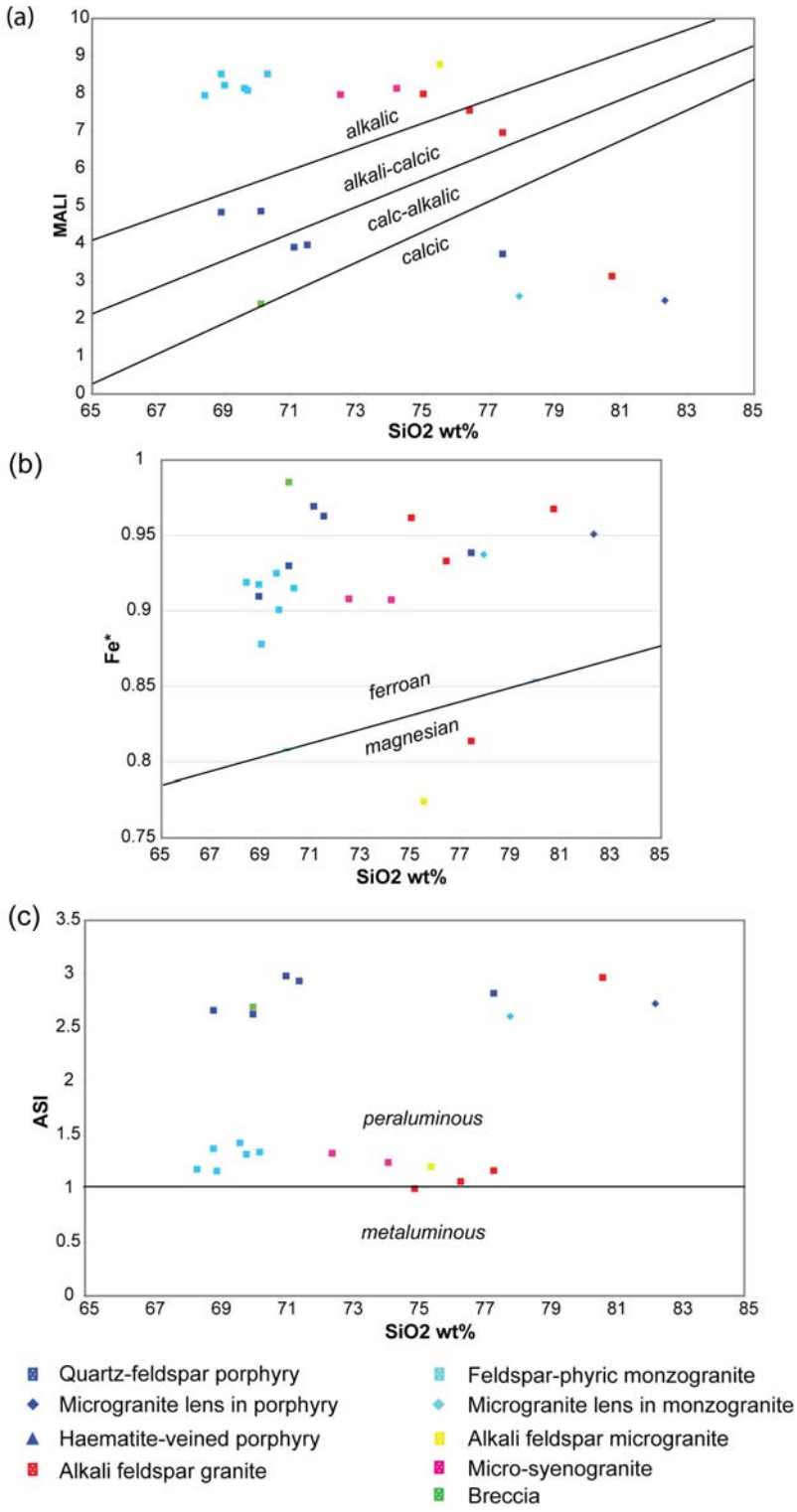

Figure 21. MALI, Fe* number and ASI classification diagrams of the Cultana Subsuite. After Frost et al., (2001).

which has a similar negative MREE anomaly suggested that this feature is caused by fractional crystallisation of the granite from a more mafic titanite – bearing parent. Future isotopic analysis may aid in clarifying the likelihood of a mantle component to the Cultana Subsuite.

Economic elements

Limited exploration has been carried out in the Cultana Inlier, but a compilation of company rock chip geochemical assays (Fig. 22) indicate that the Cultana Subsuite is anomalous in a number of elements typically associated with IOCG – style mineralisation, with best values of 53 ppb Au and 1300 ppm Cu and elevations in iron (39% FeO), U (59 ppm) REE (La 1240 ppm), Ba (1350 ppm), Pb (95 ppm) and Zn (220 ppm), implying that the hydrothermal fluids responsible for alteration of the Cultana Subsuite carried some metals.

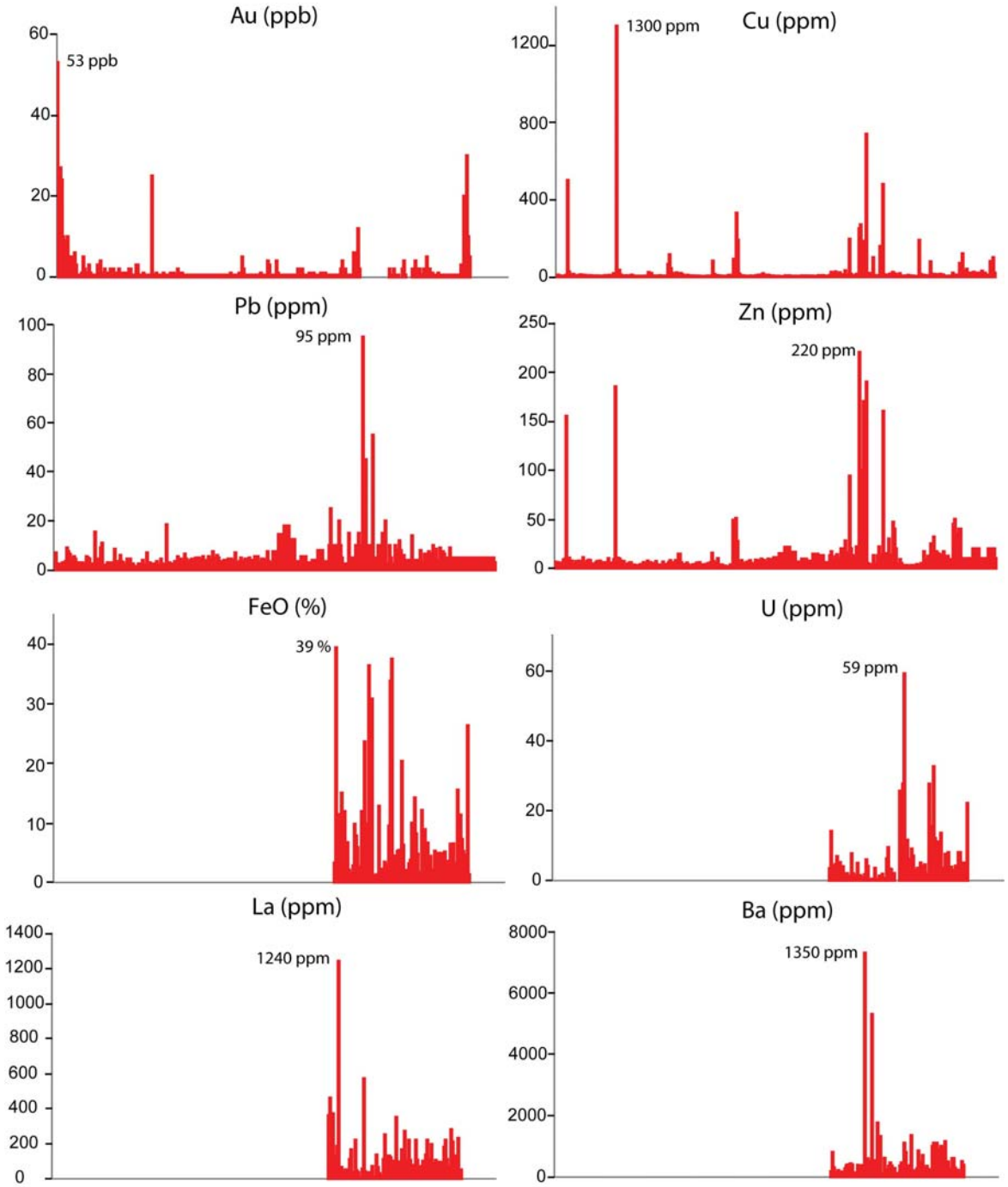

Figure 22. A selection of economic element values from rock chip samples of the Cultana Subsuite. Gaps in the data indicate that the sample was not assayed for the shown element. Compiled from Craton Resources and Normandy data in Env 9596 (Craton Resources, 2001), and samples from the Geological Survey Branch database SAGEODATA collected by S.O. McAvaney, A.J. Parker, and G. Ferris (accessed through https://info.pir.sa.gov.au/geoserver/sarig/frameSet.jsp).

GEOPHYSICAL SIGNATURE OF THE CULTANA INLIER

The Cultana Inlier has a complex magnetic response (Fig. 23). The western margin of the inlier which is bound by the Cultana Fault is marked by an abrupt contact with the bland low magnetic signature of the Neoproterozoic sediments in the Stuart Shelf. The eastern margin of the inlier extends below the coastline of the Spencer Gulf, and is similarly defined by an abrupt contact with the bland magnetic signature of sedimentary cover of Cainozoic sedimentation in the Pirie Basin and Spencer Gulf overlying the Torrens Hinge Zone.

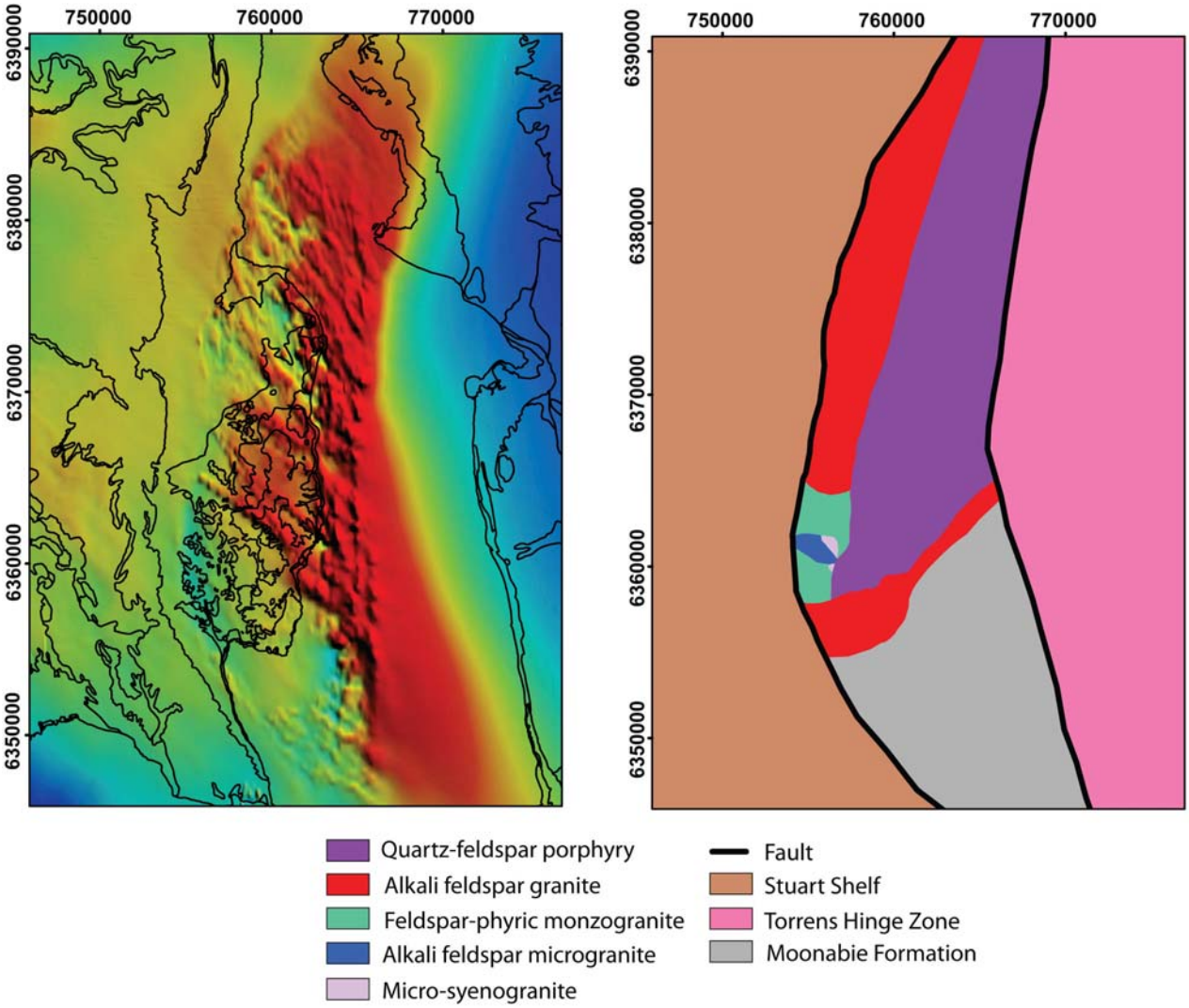

Figure 23. Magnetics image of the Cultana Inlier (PIRSA state magnetics dataset) overlain by 100K geology

The inlier is characterised by two magnetic domains: a low and bland magnetic signature in the southern part of the inlier, and a domain characterised by high magnetic linear features in the northern part of the inlier. The outcropping contact between the Cultana Subsuite and the Moonabie Formation has no magnetic response, and there is no observable difference in the lithology or alteration style of the Cultana Subsuite across this domain boundary.

The Cultana Subsuite is characterised by a low magnetic susceptibility (Table 1), which is reflected in the low magnetic signature of the southern domain in the inlier. The northern part of the inlier is defined by linear magnetic features with two principal orientations, SSE–NNW and SE–NW, and a number of the SSE-NNW features appear to cross-cut the SE–NW features. The magnetic response is highest along the eastern edge of the inlier. The trend of the high magnetic features does not reflect the dominant trend of fracturing and veining observed in the Cultana Subsuite and Moonabie Formation (Fig. 16). Craton Resources suggested that these NW structures coincide

Table 1. Magnetic susceptibility values of the Cultana Subsuite.
Units x 10^{-5} SI.

Lithology	Minimum	Maximum	Average	Measurements
Mu1	2.2	17.8	8.8	4
Mu2	8.4	18.6	12.8	3
Mu3	2.6	55.6	19.6	7
Mu4	0	9	2	7
Mu5	7	14	10.5	2

with haematite – sericite – epidote alteration zones (Craton Resources, 2001). However, these features most likely represent the Gairdner Dolerite dyke swarm whose high magnetic response is also observed to the west and northwest of the inlier beyond the Simmens Plateau, but is dampened immediately to the west beneath the Stuart Shelf. The magnetic high on the eastern edge of the inlier may in part be Beda Volcanics, to which the Gairdner Dolerite dykes are believed to be feeders, and which are exposed on the eastern and southern margin of the inlier.

TECTONISM OF THE CULTANA INLIER

The dominant N–S to NNE–SSW orientation of veining in the Cultana Subsuite suggests that the maximum extension axis of the local area at the time of veining, and at least late stage alteration given that the veins host haematite alteration, was orientated E–W to ESE–WNW. The orientation of principle structures at Olympic Dam differs, where the long axis of the haematite breccia is WNW–ESE, and is dominated by WNW–ESE and NNW–SSE faults (Reeve et al., 1990), and at Prominent Hill where the dominant structural trend is NW and NE, expressed by crustal-penetrating structures visible in the geophysics and lower order structures controlling grade variations (Belperio and Freeman, 2004).

It is evident that the faults bounding the Cultana Inlier have been active during a number of events (Fig. 24). The first episode of uplift may have occurred at ~1590 Ma coeval with the crystallisation and alteration of the Cultana Subsuite. Given that the age of crystallisation and mineralisation of haematite-dominant IOCG systems hosted in Hiltaba Suite granitoids such as Olympic Dam are indistinguishable (Skirrow et al., 2007) and that alteration and mineralisation occurred in a near – surface environment, it is believed that the plutons were unroofed immediately after intrusion, (Reeve et al., 1990). The depth of alteration relative to the depth of crystallisation at Cultana is not known, but the sub-volcanic petrological textures suggest a shallow intrusion depth, and the alteration is brittle and contains some epithermal characteristics, such as the haematite – quartz filled breccia cavity, also suggesting a shallow depth. Similarly, evidence for Mesoproterozoic unroofing exists at Oak Dam and Acropolis prospects, which are unconformably overlain by the Mesoproterozoic fluvial Pandurra Formation (Preiss, 1987; Davidson et al., 2007).

Uplift of the Cultana Subsuite to the surface may have also occurred in the Mesoproterozoic prior to deposition of the Pandurra Formation, which is absent on the Cultana Inlier, due either to lap out along the eastern margin of the Cariewerloo Basin, or subsequent erosion (Preiss, 1987). Uplift had certainly occurred prior to deposition of the Backy Point Formation, a fluvial sandstone (Cowley, 1991) which unconformably overlies the Cultana Subsuite at Cultana and Solution Hills and Douglas Point (Fig. 3). The Backy Point Formation is interlayered with the Beda Volcanics, an amygdaloidal basalt, which has yielded variable Rb-Sr ages of 697 ± 70 Ma (Webb and Hörr, 1978), which is younger than the Rb-Sr age of the overlying Tapley Hill Formation, 750 ± 53 Ma (Webb and Coats, 1980), and 1076 ± 34 Ma (Webb and Coats, 1980). It is believed to be equivalent to the Gairdner Dolerite dykes (Mason et al., 1978) which date to 827 ± 6 Ma (Wingate et al., 1998), and the Arkaroola Subgroup volcanics in the Adelaide Geosyncline (Preiss, 1987).

The Cultana Fault is interpreted to have been active as a growth fault in the Neoproterozoic during deposition of the sediments of the Stuart Shelf during the Torrensian and early Sturtian (Preiss, 1987). Some time after the deposition of the Marinoan Tent Hill Formation the Cultana Fault was reactivated as a reverse fault, and the Umberatana and Wilpena Group sediments which would have overlain the Cultana Inlier were eroded at this time. At Old Point Lowly, the Cultana Fault

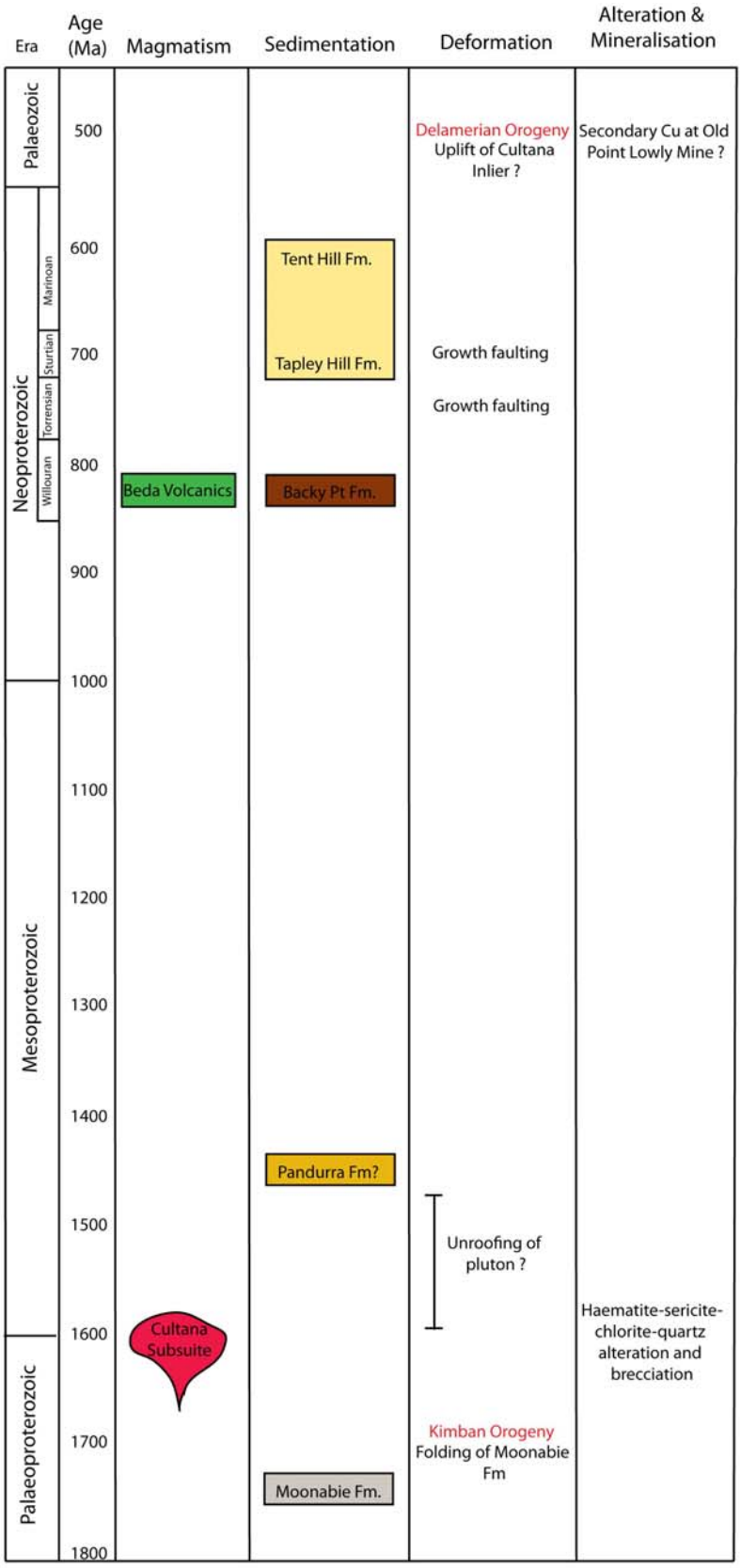

Figure 24. Geological timeline of the Cultana Inlier

displaces Beda Volcanics on the east against the younger Tapley Hill Formation on the west (Mason, 1980). Secondary copper mineralisation is present within the fault zone and at the unconformity between the Tapley Hill Formation and Beda Volcanics on the eastern side (Mason, 1980). This faulting event may have occurred during the Delamerian Orogeny (Preiss, 1987), which caused folding and faulting in the Adelaide Geosyncline across the Spencer Gulf, and faulting in the Torrens Hinge Zone, the western margin of which lies close to the eastern edge of

the inlier beneath the Spencer Gulf. The eastern fault to the Cultana Inlier marks the western boundary of the Spencer Gulf, and is likely to have been active in the Tertiary, during which time deposition of sediments was effected by the reactivation of older structures (Gostin et al., 1984).

SIGNIFICANCE OF ALTERATION AND BRECCIATION IN THE CULTANA INLIER

The nature of the alteration and brecciation of the Cultana Subsuite shares many similarities with other IOCG systems in the Gawler Craton, particularly Olympic Dam and Prominent Hill. The principal alteration minerals at Olympic Dam and Prominent Hill are haematite – sericite – silica – chlorite (Table 2), which are also present at Cultana, although chlorite is only a minor feature. In many instances the alteration takes a similar form, such as haematite replacing primary igneous minerals and occurring as polymetallic veins, feldspar altered to sericite and tourmaline – quartz ± chlorite veins in the granite and granite – rich breccia, which occur at Olympic Dam (Reeve et al., 1990) and are similar to the alteration style observed at Cultana. Similarly, at Prominent Hill pervasive earthy haematite alteration occurs in rocks adjacent to mineralised breccias, and are cut by late stage haematite veinlets (Belperio et al., 2007), not dissimilar to the haematite alteration observed at Cultana. However, other alteration minerals at Olympic Dam and Prominent Hill, such as barite, carbonate and fluorite, are not observed as part of the exposed alteration of the Cultana Subsuite.

Table 2. Alteration mineralogy of selected IOCG systems in the Gawler Craton. Compiled from Reeve et al., (1990), Reynolds, (2001), Belperio and Freeman, (2004), Belperio et al., (2007).

	Olympic Dam	Prominent Hill	Cultana Inlier
Haematite	x	x	x
Magnetite	x		
Sericite	x	x	x
Silica	x	x	x
Chlorite	x	x	x
Carbonate	x	x	
Barite	x	x	
Tourmaline	x		x
Fluorite	x	x	
Feldspar			x

There are also similarities with particular zones of brecciation in these IOCG systems (Table 3). The Olympic Dam deposit is hosted within the Hiltaba age Roxby Downs Granite, and is zoned from weakly altered and fractured granite at the periphery of the deposit, to weakly brecciated granite, granite breccia with a haematite matrix, heterolithic breccia of granite and haematite clasts, haematite breccia, to a haematite – quartz breccia core in the centre of the deposit (Reynolds, 2001). The heterolithic and haematite breccias host most of the mineralisation as disseminated grains, veinlets and fragments in breccia zones, primarily within the breccia matrix (Reeve et al., 1990). Similarly, the Prominent Hill deposit is hosted within the Gawler Range Volcanics and associated sediments and contains varying degrees of alteration and brecciation, from a broad zone of iron oxide – sericite alteration, weakly brecciated host rock, clast-supported jigsaw breccia (<2% matrix), matrix-supported jigsaw breccia (15–50% matrix) and matrix supported heterolithic breccia (up to 90% matrix) and a barren Fe-Si-Ba core (Belperio et al., 2007). At Cultana only weakly fractured and altered granite and porphyry are observed, containing localised areas of brecciation and more intense alteration. This level of alteration and brecciation is equivalent to the lower intensity unmineralised periphery of the Olympic Dam and Prominent Hill deposits.

There are a number of different possibilities as to what the alteration and brecciation observed at Cultana represents. It may be that Cultana has been affected by only a barren iron – rich system which was lacking in one or more of the features required for IOCG – style mineralisation (Oreskes and Einaudi, 1992; Haynes, 1995; Oliver et al., 2004; Skirrow et al., 2006; Skirrow, 2008) such as:

Table 3. Degrees of brecciation in selected IOCG systems in the Gawler Craton. Compiled from Reeve et al., (1990), Reynolds, (2001), Belperio and Freeman, (2004), Belperio et al., (2007).

	Olympic Dam	Prominent Hill	Cultana Inlier
Host Rock	Roxby Downs Granite	Gawler Range Volcanics & sediments	Cultana Subsuite
Periphery of alteration system	Weakly altered and fractured granite	Broad zone Fe oxide – silica alteration	Altered and fractured quartz-feldspar porphyry
	Granite breccia with haematite matrix	Weakly brecciated host rock and clast-supported jigsaw breccia (<2%)	Micro-granite breccia with haematite matrix
↓	Heterolithic breccia of granite and haematite clasts	Matrix- supported jigsaw breccia (15–50%)	Not observed
	Haematite-rich breccia	Matrix-supported heterolithic breccia (≤90%)	Not observed
Core of alteration system	Haematite-quartz breccia core	Fe-Si-Ba core	Not observed

- a metal source
- a sulphur source
- correct fluid geochemistry
- mafic magmatism
- structural control
- hydrothermal brecciation intensity
- palaeodepth of formation and igneous setting.

In particular the absence of mafic magmatism at Cultana may be significant, as many genetic models of IOCG deposits suggest that mafic magmatism is an important component in ore genesis as a source of metals and magmatic fluids (Reeve et al., 1990; Johnson and McCulloch, 1995; Mathur et al., 2002), and is present at Olympic Dam (Reeve et al., 1990) and Prominent Hill (Belperio and Freeman, 2004; Belperio et al., 2007). The comparison of Nd isotope data from copper mineralisation from Olympic Dam with that from barren and weakly mineralised prospects elsewhere in the Olympic Cu-Au-(U) Province indicate that the Nd in Olympic Dam has a more primitive signature, suggesting greater input from mafic and/or ultramafic rocks or magmas (Skirrow et al., 2007). Although there are no mafic lithologies observed in the surface exposure of the Cultana Subsuite, mafic members may be present at depth in the system. Alternatively, higher intensity brecciation equivalents to the mineralised haematite – rich breccias at Olympic Dam and Prominent Hill exist at depth in the system, yet to be discovered.

APPENDIXES

1. Exploration of the Cultana Inlier

SEREM AUSTRALIA 1970-1971

An Exploration licence over the Cultana Inlier was held by Serem Australia Pty Ltd between 09/04/1970 and 17/04/1971 (Serem Australia Pty Ltd, 1971). Exploration targeted copper porphyry style mineralisation in the Cultana Subsuite, and focussed at two locations where traces of copper mineralisation were found at the surface. At Old Pt Lowly mine malachite concretions were found within the rubble of a well, and a strongly altered granitic rock with veins of haematite was observed in the tailings of the old mine. At Old Well, ~34 km south of Port Augusta, malachite concretions were found in the tailings of the old well.

Initial work on the lease consisted of stream sediment and soil sampling at 182 locations, covering the whole of the inlier. Fourteen stream sediment samples contained greater than 30 ppm Cu, with anomalies located at Old Well and north-west of Douglas Point. Ten soil samples contained greater than 30 ppm, with the highest being 36 ppm. A small number of rock chip samples were collected along the east of the inlier. Unaltered porphyry 5 km south-southwest of Two Hummock Pt assayed 32 ppm Cu and 1.7% Fe , slightly altered porphyry at Monument Hill assayed 50 ppm Cu and 13.6% Fe, and completely ferruginised porphyry with quartz and haematite veining at Monument Hill assayed 1600 ppm Cu with 12.1% Fe.

Further work focussed in the vicinity of Old Point Lowly, including soil sampling and trenching, which had a highest assay of 3000 ppm Cu and 53.1% Fe. Resistivity and magnetic surveys were conducted at Old Point Lowly to locate the fault at depth. Three holes were drilled, two in the vicinity of Old Point Lowly Mine and the third ~8 km to the south. The holes at Old Point Lowly intersected diorite which is locally fractured and contains quartz veins and traces of pyrite and chalcopyrite, probably belonging to the Beda Volcanics or Gairdner Dolerite. The hole to the south intersected kaolinised basement containing traces of pyrite.

Serem concluded that the copper mineralisation at Old Point Lowly mine extends ~350 m south of observed surface indications, and 8 km south of observed indications at Old Well. They likened the nature of the mineralisation to that at Moonta – Wallaroo.

DEPARTMENT OF MINES 1972

The tin potential of the Cultana Subsuite was assessed by the Department of Mines in the 1970s (Sibenaler, 1972). Over 60 rock samples were collected from a range of different lithologies, including coarse grained granite, quartz porphyry, and altered granitoid with tourmaline clots. Twenty seven samples were assayed for a suite of economic elements but no significant anomalies were found, and a summary of the analyses is shown in Table 4. The higher tin values (greater than 5 ppm) are largely confined to outcrops of granite ENE of Cultana H.S. One hundred stream sediment samples were collected from the streams draining the outcropping Cultana Subsuite, but contained only low values of the elements analysed.

NORMANDY EXPLORATION LTD 1993

Normandy Exploration held an exploration licence over the Cultana inlier in 1993. The data for the licence was not released as PIRSA open file data, but is compiled in Appendix A of Craton Resources, (2001). Normandy collected soil samples over the southern and northern ends of the inlier, BLEG stream sediment samples in the south and west of the inlier, and isolated rock chip samples, which are summarised in Table 5.

Table 4. Summary of rock sample assay results of Sibenaler's study

Element	Average concentration (ppm)	Range
Pb	4	1–5
Co	5	5–20
Ni	7	5–40
V	45	20–100
Mn	106	40–300
Nb	37	<20–150
Be	5	1–15
Zr	457	100–200
Cu	18	5–120
Sn	4	1–60
B	63	5–80
Li	27	1–5
Zn	<20	–
W	<50	<50–400
Mo	3	<3–30

Table 5. Best values of Normandy Exploration rock chip assay results

Sample No	Cu (ppm)	Fe (%)	Mn (ppm)	Pb (ppm)	Zn (ppm)	Cr (ppm)	Ba (ppm)	Ce (ppm)	La (ppm)	Au (ppb)	U (ppm)
191106	24	39.40	720	25	17	40	800	650	460	<2	14
191115	480	9.45	2300	15	160	230	610	25	20	<2	0.62
191136	195	9.75	1680	15	94	210	430	45	20	14	0.72
191166	740	30.8	880	45	190	280	590	10	40	0	4.05

CRATON RESOURCES 1999–2001

The Point Lowly E.L. 2478 was held over the Cultana Inlier by Craton Resources (2001) from 09/01/1998 to 07/01/2001. Exploration targeted Cu–Au–U–REE mineralisation associated with the 'Cultana granite'. Initial work on the licence consisted of the production of 1:40 000 geomorphological and structural element maps interpreted from aerial photos. Mapping was carried out at 1:10 000 on the southern and eastern edges of the Cultana Subsuite, with particular focus on alteration and structure. They observed that north-westerly structures evident in the magnetics correlate with large haematite–sericite–epidote alteration systems at the surface.

Different sampling media were trialled to find that best suited to the transported cover in the area. 629 MMI soil samples were collected on 200–400 m spaced E–W lines over targets identified from structural interpretation and field mapping in the vicinity of Cultana Homestead, Crag Point, Old Point Lowly, Monument Hill and Long Dam. Rock chip samples were collected in the southern and eastern edges of the Cultana Complex, and are summarised in Table 6. Due to continuing difficulties in obtaining access within the Cultana Army Training Area the licence was surrendered.

Table 6. Best values of Craton Resources assay results

Sample No.	Au (ppb)	Au (dup)	Co (ppb)	Mo (ppb)	Ni (ppb)	Cd (ppb)	Zn (ppb)	Ag (ppb)	As (ppb)	Bi (ppb)	Cu (ppb)	Pb (ppb)	U (ppb)
C2	53	32	1.1	4.7	5	0	6.5	0.05	6.0	6.0	5.0	3.0	0.5
C3	24	33	0.3	0.5	0	0	2.5	0.10	19.0	12.5	9.5	7.0	0.8
C12	3		17	6.5	61	0.1	155.0	0	48.0	1.1	500.0	3.5	45.0
C56	2		3200	190.0	320	0.9	185.0	1.55	19.5	44.0	1300.0	8.5	9.5
C80	25	21	2.1	60.0	11	0.2	7.5	0.05	25	4.6	23.5	7.0	11.5
C248	5	8	51.0	2.2	79	0	51.0	0	1.0	120.0	330.0	7.0	5.5

2. Pontifex and Associates Mineralogical Report No. 9230 by Alan C. Purvis, PhD

SUMMARY COMMENTS

Ten previously prepared thin sections are described in this report. These are listed below together with the header from each description as an overall summary of the individual petrographic descriptions.

The provided thin sections mostly represent partly altered granitoids varying from monzogranite to alkali feldspar granite, (using IUGS quartz-alkali feldspar-plagioclase rock classification). Sample R1562801 however is highly altered and may be classified as greisen or sericite-quartz-altered granitoid. Samples (R1562802 and 803) seem to represent altered quartz-rich sandstones.

The granitoids commonly contain muscovite, with altered possible biotite in some samples, tourmaline in two samples and only generally sparse zircon (most abundant in R1562801). Altered plagioclase, where present, seems to have been partly fritted and filled with inclusions of granophyre or occurs as shells within, and rims around, alkali feldspar phenocrysts in a rapakivi-like arrangement. These occurrences are similar to some plagioclase phenocrysts in Gawler Range Volcanics. Several samples have abundant granophyre indicating a probable subvolcanic genesis and indeed, this granitoid suite as a whole may represent subvolcanic intrusives.

The two probable sandstones contain sericite and rare small mostly rounded zircons. These are of uncertain origin and stratigraphic age.

1. R1562779: Alkali feldspar granite with muscovite, clay, tourmaline, rutile, zircon and fluorite.
2. R1562780: Sericitised granitic porphyry with magnetite, possible rutile and patches of muscovite possibly ex-biotite.
3. R1562782: Weakly granophyric alkali feldspar granite porphyry with tourmaline and rare zircon: weakly hematite-stained.
4. R1562784: Granophyric monzogranite with albite-sericite-clay-hematite alteration, albite in fractures and minor oxide, apatite and zircon.
5. R1562785: Hematite-stained, partly sericitised, partly rapakivi-like granophyric monzogranite with opaque oxide and rare zircon.
6. R1562792: Weakly porphyritic alkali feldspar microgranite with altered plagioclase phenocrysts and rare quartz phenocrysts.
7. R1562796: Altered microsyenogranite with sericite ± hematite ex-plagioclase and hematite-stained K-spar: partly granophyric.
8. R1562801: Greisen, formerly quartz-feldspar-porphyritic, with sericite-hematite-quartz-leucoxene alteration and relatively abundant zircon in and adjacent to magnetite (possibly oxidised?). The feldspar phenocrysts seem to be partly fritted or rapakivi-like.
9. R1562802: Quartz-rich poorly sorted very coarse-grained sandstone (or greisen?) with abundant hematite-stained sericite and minor opaque oxide ± leucoxene. Rare zircon is present.
10. R1562803: Quartz-rich coarse-grained sandstone with interstitial sericite and hematite, sparse zircon and hematite veins.

INDIVIDUAL DESCRIPTIONS

Sample ***R1562779***

Rock name Alkali feldspar granite with muscovite, clay, tourmaline, rutile, zircon and fluorite.

Petrography

A visual estimate of the modal mineral abundances:

Mineral	Vol %	Origin
Orthoclase (perthitic)	63	Igneous
Quartz	29	
Plagioclase	3.5	
Muscovite and clay	3	Deuteric and secondary
Oxide and rutile	1	Primary
Tourmaline	0.5	Possibly deuteric
Zircon	Trace	Accessory to 0.5 mm
Fluorite	Trace	Secondary/deuteric

Perthitic orthoclase dominates this sample with anhedral grains to 10 mm long partly interstitial to less abundant quartz to 8 mm in grainsize. Some of the quartz has crystal faces and some ahs resorption channels filled with orthoclase, suggesting subvolcanic emplacement. Minor plagioclase is disseminated as small subhedral crystals but there are also patches of muscovite and clays containing oxidised opaque oxide, leucoxene or rutile and minor zircon as partly fractured grains to 0.5 mm long. One patch also contains sparse blue fluorite.

Sample ***R1562780***

Rock name Sericitised granitic porphyry with magnetite, possible rutile and patches of muscovite possibly ex-biotite.

Petrography

A visual estimate of the modal mineral abundances:

Mineral	Vol %	Origin
Sericite ex-feldspar phenocrysts	51	Ex-feldspar phenocrysts
Quartz phenocrysts	23	Primary
Quartz-sericite ex groundmass	23	Partly altered groundmass
Oxide	2	Primary
Muscovite	1	Secondary

This sample is sericitised granitic porphyry with abundant sericitised feldspar phenocrysts from 0.4–4 mm long and less abundant quartz phenocrysts, to 6 mm in diameter, commonly rounded and resorbed. The groundmass was formerly quartzofeldspathic and has fine-grained granular quartz and sericitised former feldspar. Small phenocrysts of partly oxidised magnetite are as much as 1.5 mm in diameter, with very minor possible rutile. Patches of decussate muscovite may have replaced former biotite and there are narrow quartz-filled fractures to 0.4 mm wide.

Sample ***R1562782***

Rock name Weakly granophyric alkali feldspar granite porphyry with tourmaline and rare zircon: weakly hematite-stained.

Petrography

A visual estimate of the modal mineral abundances:

Mineral	Vol %	Origin
K-spar (phenocrysts and groundmass)	41	Igneous
Quartz phenocrysts	20	
Groundmass quartz	22	
Granophyre	13	
Plagioclase	1.5	
Tourmaline	2	Deuteric/pneumatolytic?
Oxide, rutile	0.5	Primary
Zircon	Trace	Accessory

This sample is also porphyritic but has quartz as phenocrysts to 6 mm in diameter, commonly rounded or with a volcanic or subvolcanic appearance and less abundant K-spar phenocrysts to 8 mm in diameter. There is also a groundmass with a mixture of separate inequigranular quartz and K-spar as well as aggregates of granophyre ranging from quartz-poor to quartz-rich, to 2 mm in diameter. The K-spar is pale reddish with hematite staining. The texture is to some extent seriate or inequigranular in character with all variations from fine-grained to the size of small phenocrysts, including K-spar to 4 mm long. Plagioclase is sparse and occurs partly as inclusions in orthoclase phenocrysts, where it is rimmed by graphic quartz, as well as in the groundmass with weakly sericitised laths to 2 mm long. Tourmaline occurs as poikilitic grains to 4 mm in diameter and is dark greenish brown in colour. Oxides seem to be partly primary, albeit possibly oxidised, and partly secondary, with limonite ± hematite in small irregular patches. There is also sparse zircon to 0.2 mm in grainsize. It is probably best described as a weakly granophyric alkali-feldspar granite porphyry.

Sample ***R1562784***

Rock name Granophyric monzogranite with albite-sericite-clay-hematite alteration, minor oxide, apatite and zircon and albite in fractures.

Petrography

A visual estimate of the modal mineral abundances:

Mineral	Vol %	Origin
Largely sericitised plagioclase	30	Igneous
Granophyre	61	
Granular late magmatic quartz	5	
Rounded ‘phenocryst’ quartz	1.5	
Oxide and leucoxene	2	
Muscovite and clay	0.5	Secondary
Apatite, zircon	Trace	Accessory

The bulk mineralogy of this sample suggests granophyric monzogranite with more abundant plagioclase compared to the previous samples. The plagioclase is largely sericitised and albitised and is inequigranular with one grain more than 10 mm long and 10 mm wide, extensively fritted with inclusions of granophyre and oxidised magnetite ± leucoxene. The other crystals are mostly less than 6 mm long with albite-sericite alteration and inclusions of K-spar ± quartz in a graphic texture and patches of secondary earthy hematite. The bulk of the rock is composed of relatively large granophyre patches, to 3 mm in diameter, with scattered patched of apparently late magmatic quartz that are commonly optically continuous with quartz in one of the adjacent patches of granophyre. The largest patch is 5 mm in maximum diameter and is polycrystalline. There are also rounded quartz grains that would be classified as phenocrysts in a finer-grained host rock and seem to be of early magmatic origin with resorption as the magma reached higher levels in the crust. Minor components are oxidised opaque oxide and leucoxene, with needles of apatite to 1 mm long and various muscovite-clay-hematite aggregates. Clouded possible zircon is present, from 0.1–0.3 mm long. There are also fractures filled with albite.

Sample ***R1562785***

Rock name Hematite-stained, partly sericitised, partly rapakivi-like granophyric monzogranite with opaque oxide and rare zircon.

Petrography

A visual estimate of the modal mineral abundances:

Mineral	Vol %	Origin
Sericite-hematite ± albite ex-plagioclase	29	Igneous, partly altered
Granophyre between ex-plagioclase	43	
Granophyre within ex-plagioclase	5.5	
K-spar ± kaolinite rimmed by ex-plagioclase	15	
Oxide ± leucoxene	2	
Granular late magmatic quartz	5.5	
Zircon	Trace	

This sample seems to be related to the previous sample and has sericite-hematite-altered plagioclase as phenocrysts that are highly fritted and contain abundant internal granophyre patches with a weaker hematite staining. Others, to 10 mm long and 6 mm wide, have cores of probable K-spar, commonly with patches of probable kaolinite, and sericite-hematite-altered plagioclase as zones and rims, locally accompanied by granophyre and opaque oxide. Interstitial granophyre to 3 mm in diameter is also abundant as in the previous sample and has patches of apparently late magmatic quartz that is usually optically continuous with quartz in one of the adjacent granophyre patches. Rare zircon was seen, 0.1 mm in grainsize, and there is disseminated possibly oxidised magnetite, rarely more than 0.5 mm in diameter. Irregular hematite ± clay staining is widespread. This sample again seems to represent granophyric monzogranite but has some rapakivi characteristics.

Sample ***R1562792***

Rock name Weakly porphyritic alkali feldspar microgranite with altered plagioclase phenocrysts and rare quartz phenocrysts.

Petrography

A visual estimate of the modal mineral abundances:

Mineral	Vol %	Origin
Sericite ex-plagioclase phenocrysts	3	Ex-plagioclase phenocrysts
Quartz phenocrysts	1	
Groundmass quartz	35	Primary igneous
Groundmass plagioclase	2	
Groundmass K-spar	55–60	
Muscovite, hematite and altered biotite	2	Secondary

This sample is mostly composed of a fine granular groundmass of quartz and slightly reddish K-spar, mostly from 0.1–0.5 mm in grainsize, but there are sparse sericitised anhedral plagioclase grains to 3 mm long and less abundant elliptical quartz phenocrysts to 3 mm long. Small amounts of oxide, muscovite and altered biotite occur but no zircon was seen. The composition indicates alkali feldspar microgranite.

Sample ***R1562796***

Rock name Altered microsyenogranite with sericite ± hematite ex-plagioclase and hematite-stained K-spar: partly granophyric.

Petrography

A visual estimate of the modal mineral abundances:

Mineral	Vol %	Origin
Sericite ± hematite ex-plagioclase	7–8	Igneous
Quartz, partly in granophyre	40	
K-spar, partly in granophyre	50–55	
Clays, muscovite and hematite	Trace	Secondary

This sample has sericite ± hematite-altered probable plagioclase in a groundmass of quartz and alkali feldspar, partly granular but more abundantly in granophyric aggregates to 2 mm in diameter as well as minor clay, muscovite and hematite. Some of the plagioclase has inclusions of quartz, partly as graphic intergrowths, but some may represent phenocrysts. This seems to represent altered microsyenogranite.

Sample ***R1562801***

Rock name Greisen, formerly quartz-feldspar-porphyritic, with sericite-hematite-quartz-leucoxene alteration and relatively abundant zircon in and adjacent to magnetite (possibly oxidised?). The feldspar phenocrysts seem to be partly fritted or rapakivi-like.

Petrography

A visual estimate of the modal mineral abundances:

Mineral	Vol %	Origin
Sericite-quartz-altered composite feldspar phenocrysts and dense sericite ex-feldspar	39	Ex-feldspar phenocrysts
Hematite-rich altered feldspar phenocrysts with sericite and quartz	14	Ex-feldspar phenocrysts
Quartz phenocrysts	6.5	Resorbed phenocrysts
Poorly defined quartz-sericite ex-groundmass material	37	Groundmass
Magnetite and leucoxene-sericite aggregates with minor zircon	3.5	Igneous, partly altered

This sample is highly altered, possibly with phyllic or greisen-like alteration but has rounded resorbed quartz phenocrysts to 4 mm in diameter and has apparently fritted or rapakivi-like feldspar phenocrysts as seen in R1562784-785, to 10 mm long, with rims of sericitised plagioclase and cores that seem to be rich in quartz, with sparse sericite, and seem to have replaced K-spar. Smaller phenocrysts seem to have been replaced by sericite with little or no quartz. Other feldspar phenocrysts are more euhedral and replaced by sericite and hematite in various proportions. The groundmass is poorly preserved and has various proportions of quartz and sericite in different areas, with no clear evidence as to the original mineralogy or texture. Granular magnetite is present, to 1 mm in grainsize, as well as opaque oxide altered to sericite with a trellis like arrangement of leucoxene or anatase representing former ilmenite lamellae. Zircon is more abundant than in the previous samples and occurs as crystals from 0.1–0.4 mm long, mostly in and adjacent to magnetite grains. The original composition is uncertain and the rock is best classified as greisen.

Sample ***R1562802***

Rock name Quartz-rich poorly sorted very coarse-grained sandstone (or greisen?) with abundant hematite-stained sericite and minor opaque oxide ± leucoxene. Rare zircon is present.

Petrography

A visual estimate of the modal mineral abundances:

Mineral	Vol %	Origin
Quartz	70	Possibly detrital
Sericite, hematite-stained	25–30	Interstitial
Hematite and leucoxene	2–3	Possibly detrital
Zircon	Rare	Accessory

This sample has abundant rounded to amoeboid quartz grains from 0.1–2 mm in grainsize with interstitial decussate sericite, stained with hematite, and disseminated granular opaque oxide, accompanied by leucoxene/anatase. Zircon 0.15 mm in grainsize is partly rimmed by anatase. This sample could be a greisen derived from a fine-grained granitoid but a very coarse-grained quartz-rich sandstone is more probable as there is no obvious igneous texture. Lenses of recrystallised quartzmay represent disrupted veins.

Sample ***R1562803***

Rock name Quartz-rich coarse-grained sandstone with interstitial sericite and hematite, sparse zircon and hematite veins.

Petrography

A visual estimate of the modal mineral abundances:

Mineral	Vol %	Origin
Quartz	50	Detrital?
Sericite	35	Interstitial
Hematite (disseminated)	3	Interstitial
Hematite (in veins)	10–15	Hydrothermal
Zircon	Trace	Detrital?

Rounded to lobate quartz grains in this thin section are mostly more than 0.2 mm in diameter and rarely more than 1 mm, suggesting coarse-grained sandstone. Some areas have closely packed quartz grains with stylolitic grain boundaries but other areas have abundant interstitial sericite, weakly hematite-stained compared to the previous sample, with small patches of earthy ± crystalline hematite. A patch of crystalline hematite, 3 mm in diameter, encloses some quartz, and there are veins to 2 mm wide with crystalline hematite and less abundant earthy hematite, commonly irregular in outline with lenses of fine-grained quartz. Zircons from 0.05 mm to 0.1 mm long are disseminated, with several in a small aggregate, and seem to be rounded.

3. Other petrological descriptions

Sample	***R20806***	***Thin section***	TS29560
Rock name	Granite		
Reference	Env1582		
Location	757036 mE	6364830 mN	GDA94

Petrography

A visual estimate of the modal mineral abundances:

Mineral	Vol %
Potassium feldspar	40–50
Plagioclase	20
Quartz	30
Tourmaline	5
Biotite	trace
Sphene	trace
Opaques	trace
Fluorite ?	trace

This is a coarse-grained granite rock, with most crystals between 5–10 mm in size. Perthitic potash feldspar is the dominant constituent and it is moderately to strongly clouded. Plagioclase is fairly extensively sericitised and occurs partly as interstitial grains, smaller than potash feldspar, and partly as broad rims or overgrowths on potash feldspar. A little quartz, possibly secondary, occurs as irregular inclusions in feldspar, but most of the quartz occurs as large, anhedral, unstained grains.

Tourmaline is unusually abundant in this rock, occurring both as numerous small grains and granular patches and as large grains, 3 mm across. The tourmaline is pleochroic with brown and blue colours. Finely granular opaques occur associated with some of the tourmaline and also with occasional flakes of pale brown biotite. Minor opaque-free biotite is also present. Other accessories are minor sphene and a little isotropic matter, possibly fluorite.

This rock is a coarse-grained granite which is slightly altered, but does not appear to have been tectonically deformed.

Sample	***R20807***	***Thin section***	TS29561
Rock name	Altered quartz – feldspar porphyry		
Reference	Env1582		
Location	759581 mE	6366006 mN	GDA94

Petrography

A visual estimate of the modal mineral abundances:

Mineral	Vol %
Quartz phenocrysts	20
Altered 'feldspar' phenocrysts	20
Matrix	60
Opaques	1

This rock is an altered quartz-feldspar porphyry, although no feldspar remains as such. The quartz phenocrysts range up to about 8 mm in size and all show rounding and embayments due to resorption. Originally there were feldspar phenocrysts, about equally abundant as quartz and with a similar size range, but these phenocrysts have been completely replaced by fine-grained clay or clay-sericite.

The matrix probably consisted originally of a granular mosaic of quartz and feldspar, with a grain size averaging 0.1–0.2 mm. No feldspar remains, however, and its place has been taken by clay or clay-sericite if the same kind as the pseudomorphed phenocrysts.

Other constituents in this rock are minor. There are small (0.3–0.5 mm) opaque phenocrysts and small opaque grains are thinly scattered through the matrix. Occasional crystals of allanite, zircon and monazite are also present in the matrix.

Sample	***R20808***	***Thin section***	TS29562
Rock name	Altered quartz-feldspar porphyry		
Reference	Env1582		
Location	761017 mE	6365466 mN	GDA94

Petrography

A visual estimate of the modal mineral abundances:

Mineral	Vol %
Quartz phenocrysts	25
Altered feldspar phenocrysts	10–20
Matrix	

This rock is similar to R20806. It contains large (up to 16 mm) phenocrysts of resorbed quartz, together with pseudomorphed feldspar phenocrysts, now composed of clay and/or sericite. One difference between this rock and R20806 is the greater abundance of sericite (i.e. colourless, highly birefringent, fine-grained phyllosilicate) relative to clay (i.e. colourless, weakly birefringent, fine-grained phyllosilicate) in this case. In a number of instances in this rock discrete flakes (0.2 mm) of white mica have developed within patches of sericite. Opaques are also rarer in this sample than R20806, there being only a few microphenocrysts and thinly scattered small grains in the matrix. Apart from these features, this rock is very similar to R20806 and the matrix consists of granular quartz (0.05–0.1 mm) intergrown with clay and sericite.

Sample	***R20809***	***Thin section***	TS29563
Rock name	Altered quartz – feldspar porphyry		
Reference	Env1582		
Location	761611 mE	6362942 mN	GDA94

Petrography

A visual estimate of the modal mineral abundances:

Mineral	Vol %
Quartz phenocrysts	5–10
Altered feldspar phenocrysts	25
Opaques	1–2
Matrix	60–70

This rock is similar to R20807-R20808, but some differences are apparent. One notable difference is the smaller proportion of quartz phenocrysts and the larger proportion of altered feldspar phenocrysts. As in the previous cases, the quartz phenocrysts show evidence of resorption and some feldspar pseudomorphs are composed of sericite and/or clay. Most feldspar pseudomorphs, however, are composed of what appears to be secondary untwinned granular albite, heavily speckled with sericite and clay.

Opaque grains are present as small granules in the matrix, as microphenocrysts and as porous aggregates which may be altered ferromagnesian phenocrysts. Scattered euhedral grains of monazite (0.1–0.2 mm) are conspicuous, though only a very small proportion of the rock. As in the previous rocks, the matrix consists of granular quartz intergrown with sericite and clay. The quartz in the matrix is a little coarser-grained than in R20808, but is similar in size to the matrix quartz in R20807 (0.1–0.2 mm).

Sample	***R20810***	***Thin section***	TS29564
Rock name	Granophyric quartz-feldspar porphyry		
Reference	Env1582		
Location	759283 mE	6360737 mN	GDA94

Petrography

A visual estimate of the modal mineral abundances:

Mineral	Vol %
Quartz phenocrysts	5–10
Altered feldspar phenocrysts	20
Opaques	2–3
Tourmaline	1
Monazite	trace
Matrix	70

In some respects this rock is similar to those previously observed, in that it contains phenocrysts of resorbed quartz and altered feldspar. It differs, however, by having a well-developed granophyric texture in the matrix. Some feldspar phenocrysts have been completely replaced by clay, sericite, and possibly secondary albite, but in many cases some remnant primary feldspar remains, though heavily clouded. Sodium cobaltinitrite staining of the rock slab showed that potash feldspar is present both as phenocrysts and in the matrix, where it is abundant. Opaques are present as phenocrysts and as porous aggregates, which may be altered ferromagnesian phenocrysts.

Brown to blue pleochroic tourmaline is a notable feature of this rock and forms single grains and patches up to about 1 mm across. These seem to be localised along a fracture. The presence of tourmaline in this rock suggests affinities with R20806, in which tourmaline was an important constituent. A feature which this rock has in common with R20809 is the presence of conspicuous euhedral crystals of monazite.

Sample	***R20811***	***Thin section***	TS29565
Rock name	Altered granophyric rock		
Reference	Env1582		
Location	758746 mE	6358485 mN	GDA94

Petrography

A visual estimate of the modal mineral abundances:

Mineral	Vol %
Quartz	30–40
Altered feldspar	60
Tourmaline	1
Opaques	1
Sphene	trace
Monazite	trace

This rock is broadly similar to several of the preceding samples. It contains crystals of quartz, up to about 4 mm, which appear to be partly resorbed phenocrysts. Between these crystals there are patches of vernicular, optically continuous quartz. The spaces between the vernicular grains are filled with secondary material and the patches are clearly granophyric intergrowths, in which the feldspar has been altered.

In some parts of the rock there are solid patches of sericite after feldspar. Elsewhere the matrix between the quartz crystals seems to be composed of finely granular material, possibly albite, heavily speckled with clay and sericite. This is undoubtedly also altered feldspar. The rock contains a few patches of opaque or semi-opaque matter and small grains of tourmaline, mainly in clusters, are quite numerous. Occasional grains of sphene, monazite and possible allanite are present.

Sample	***R20812***	***Thin section***	TS29566
Rock name	Altered granitic rock		
Reference	Env1582		
Location	760642 mE	6357163 mN	GDA94

Petrography

A visual estimate of the modal mineral abundances:

Mineral	Vol %
Quartz	30
Altered feldspar	60–70
Tourmaline	2–3
Mica (primary)	1
Sphene	trace
Opaques	trace
Monazite	trace

This rock is composed of angular quartz grains in a fine-grained phyllosilicate-rich matrix. The quartz grains average about 1 mm in size and many are aggregated. Most of the matrix is composed of seriticte or clay, after feldspar, but in places there is fine granular material (? albite) like that in R20811. Remnants of granophyric texture are recognisable in only a few instances in this rock.

Green to blue tourmaline is a prominent constituent of this rock and occurs mainly intergrown with quartz. There is also some apparently primary mica (up to 0.6 mm) both muscovite and very pale (? leached) biotite. Opaque grains are rather rare in this rock, but small grains of dark sphene are not uncommon and there are a few crystals of monazite.

Sample	***R20813***	***Thin section***	TS29567
Rock name	Altered granophyric rock		
Reference	Env1582		
Location	759362 mE	6357043 mN	GDA94

Petrography

A visual estimate of the modal mineral abundances:

Mineral	Vol %
Quartz	30–40
Matrix	60
Opaques	1
Sphene	trace
Monazite	trace
Mica (primary)	trace

The rock contains abundant quartz, much of it with granophyric texture, in a matrix composed in part of massive sericite patches and in part of granular, apparently secondary feldspathic material, lightly to heavily speckled with sericite. Opaque or semi-opaque grains are thinly scattered through the rock and sphene and monazite are minor accessories. No tourmaline was seen. There are a few ragged flakes of muscovite which appear to be primary.

Sample	***R20814***	***Thin section***	TS29568
Rock name	Altered quartz-feldspar porphyry		
Reference	Env1582		
Location	759814 mE	6364370 mN	GDA94

Petrography

A visual estimate of the modal mineral abundances:

Mineral	Vol %
Quartz phenocrysts	10–15
Altered feldspar phenocrysts	20
Opaques	1–2
Monazite	trace
Matrix	60–70

This rock is very similar to R20807. It consists of partly resorbed quartz phenocrysts and altered feldspar phenocrysts in a matrix of granular quartz and altered feldspar. The main difference between this rock and R20807 is in the feldspar alteration, which seems much less extensive in this case, although the feldspar is still heavily clouded and sericite/clay is abundant. However, much primary feldspar remains. The rock contains a few opaque microphenocrysts and there are scattered small opaque grains in the matrix. Monazite is a minor accessory.

Sample	***R20815***	***Thin section***	TS29569
Rock name	Altered granitic rock		
Reference	Env1582		
Location	760006 mE	6363795 mN	GDA94

Petrography

A visual estimate of the modal mineral abundances:

Mineral	Vol %
Quartz	40–50
Altered feldspar	40–50
Opaques	5
Monazite	trace
Sphene	trace

This is a heterogeneous rock which contains large (6 mm) grains of quartz that appear to be phenocrysts and large massive patches of sericite that appear to be altered feldspar phenocrysts. Elsewhere there are patches of granular albite (?) and sericite and these probably also represent original feldspar phenocrysts. Between these phenocrysts there are patches of optically continuous quartz which contain seams and veins of sericite. This does not appear to be a normal granophyric texture, but it could be a related texture with a similar origin.

Opaque grains are common in this rock and range up to 2.5 mm across, although most are below 1 mm in size. Sphene is associated with some opaque grains and others contain inclusions of monazite. Euhedral crystals of monazite are actually rather common in this rock, although their total proportion is very small.

A conspicuous feature of this rock is the presence of veins which are up to about 2 mm wide but pinch out across the section. In part, the veins are composed of granular quartz but elsewhere they include opaque grains and sericite. The opaques tend to be coarse and in one place the full 2 mm width of the vein is composed of opaque matter (for a distance of at least 2 mm along the vein).

Sample	***R20816***	***Thin section***	TS24130
Rock name	Strongly altered, porphyritic, micrographic granite		
Reference	Env1582		
Location	761953 mE	6360475 mN	GDA94

Petrography

A visual estimate of the modal mineral abundances:

Mineral	Vol %
Quartz	45
Opaques	5
Sericite	45
Tourmaline	5

The rock is composed of relict phenocrysts and micrographic intergrowths of quartz embedded in a massive intergrowth of sericite, opaques and bladed crystals of tourmaline.

The quartz forms large rounded phenocrysts and finer-grained xenomorphic crystals which in places display a well-developed micrographic texture. The phenocrystal quartz is dusted with fine opaques and displays a mildly undulose extinction. Some crystals may show evidence for incipient embayment. The groundmass quartz forms irregular interlocking crystals which usually display a uniform extinction. In addition to the crystals, micrographic quartz forms a border to large blocky crystals now composed wholly of a matted aggregate of sericite. Numerous, irregular crystals of opaques have a random distribution. Bladed crystals of greenish-brown tourmaline up to 0.8 mm in diameter also occur sporadically. These have crystallised somewhat later than the relict primary mineral assemblage and are probably related to the phase of intense alteration which has affected the rock.

Relict textural features of this rock indicate it to have been a micrographic granite which has been subjected to intense pneumatolytic replacement of the feldspars by sericite and has resulted in the crystallisation of tourmaline and probably much of the opaque materials.

Sample – ***Thin section*** TS24129

Rock name Altered porphyritic ? welded tuff

Reference Env1582

Location ½ mile SSW of Douglas Point

Hand specimen description

A massive fragmental rock composed of angular to subrounded crystal fragments which range from dark grey to pale green in colour, embedded in a fine grained, reddish-grey groundmass. A few small, sub-parallel fractures along which iron oxides have precipitated traverse the rock.

Petrography

A visual estimate of the modal mineral abundances:

Mineral	Vol %
Quartz	50
Orthoclase	25
Altered plagioclase ?	10
Opaques	3
Alteration products	12

The rock is composed of large coarse-grained embayed crystals of quartz and feldspar set in a fine-grained, quartz-rich groundmass.

The quartz phenocrysts, in most cases, have a rounded habit, but a few display evidence for having crystallised with the hexagonal symmetry of high quartz. Most display cerreate margins due to embayment and all have an undulose extinction and are dusted with disseminated opaque mineral phases.

The feldspars are coarse-grained and anhedral. They form discrete crystals isolated in the finer-grained groundmass and all have been subjected to appreciable sericitisiation. Relict twinning in some cases indicates their primary composition was plagioclase of oligoclase composition. Others, however, are potash-rich and probably orthoclase.

The groundmass is composed of microcrystalline quartz, opaque minerals and sericitised potash feldspar. The quartz forms rounded crystals many of which are intergrown with the altered potash feldspar. The potash feldspar was probably orthoclase but has been subjected to partial to complete sericitisation. Opaque minerals (? Iron oxides) are ubiquitous. They form mosaic of crystals ranging up to 0.4 mm and disseminated grains occupying interstitial areas between the microcrystalline components of the groundmass.

Zircon and apatite form rare accessory components. The rock has been subjected to minor deformation and is traversed by a series of fine, sub-parallel fractures along which quartz in some instances and remobilised opaques in others have crystallised.

The rock is a porphyritic microgranite which probably represents a marginal phase to the Cultana Granite.

Sample ***A462782***
Rock name Quartz – pyrophyllite – sericite rock
Reference Env2658
Location 2600 m WNW of Backy Point

Petrography

Minerals identified microscopically: Quartz, sericite – muscovite, chlorite (little), haematite, leucoxene (titanite?)

An XRD estimate of the modal mineral abundances:

Mineral	Vol %
Quartz	35
Sericite+pyrophyllite	64
Opaques	<1

Quartz grains, mainly 300–800 μm in size, are angular, irregular in shape and don't have the appearance of normal clastic grains of sedimentary origin. Some granular aggregates are up to 1500 μm in size. Optical orientation of some groups of smaller quartz grains suggests their continuity prior to alteration.

Quartz grains are embedded in a sericite-pyrophyllite matrix; aggregates of coarser grained pyrophyllite partly invade some quartz grains. The rock has only a faint suggestion of foliation; no distinct pseudomorphs after the original rock forming minerals were found. Microscopically visible cavities and porous patches contain corroded quartz and small crystals of pyrophyllite and haematite.

The rock is a product of hydrothermal alteration of a quartz – feldspar rock, more probably a granitoid than a sediment.

Sample ***A462808***
Rock name Quartz – pyrophyllite – sericite rock
Reference Env2858
Location 2600 m WNW of Backy Point

Petrography

Minerals identified microscopically: quartz, Sericite – muscovite, tourmaline, limonite, haematite and titanite.

An XRD estimate of the modal mineral abundances:

Mineral	Vol %
Quartz	50
Muscovite-pyrophyllite	42
Tourmaline	2
Opaques	5

The rock consists predominantly of quartz grains and aggregates embedded in a sericite – pyrophyllite matrix. The shapes of some quartz grains suggest altered myrmekites. Granular aggregates of quartz are up to 3 mm in size. Hypidiomorphic to xenomorphic grains of tourmaline, partly altered to sericite, haematite and limonite. No identifiable relict texture was observed.

This is again a product of hydrothermal alteration of a feldspar-rich rock, probably a granitoid.

Sample ***A462785***
Rock name Quartz – tourmaline rock
Reference Env2858
Location 1700 m WNW of Crag Point

Petrography

Minerals identified microscopically: quartz, tourmaline, haematite, sericite and opaques.

An XRD estimate of the modal mineral abundances:

Mineral	Vol %
Quartz	53
Tourmaline	40
Sericite	3
Opaques	2

The rock consists of relatively large (in mm) hypidiomorphic grains of tourmaline and allotriomorphic grains of quartz (also in mm sizes). The quartz – tourmaline boundaries are uneven but some quartz grains have idiomorphic outlines suggesting regrowth of quartz. There is a small amount of sericite in tourmaline grains and also small interstitial patches of sericite were observed.

The rock is most probably of metasomatic origin.

Sample ***A462762***
Rock name Granite porphyry
Reference Env2658
Location 1900 m SSW of Douglas Point

Petrography

Minerals identified microscopically: quartz, sericite, opaques (leucoxene, titanomagnetite or ilmenite, haematite, limonite), titanite, tourmaline and zircon.

An XRDl estimate of the modal mineral abundances:

Mineral	Vol %
Quartz	35
Sericite	53
Opaques	10

The rock contains rounded phenocrysts of quartz up to 3 mm in size. Sericite filled fractures were observed in some phenocrysts; this and the presence of some angular fragments of quartz suggests weak cataclasis. Feldspar phenocrysts (200 µm – mm in size), completely altered to sericite, are fairly abundant. Some of them contain a considerable amount of haematite pigment. Haematite and sericite flakes are often orientated parallel to the original feldspar cleavage. Well developed, relatively large (up to 1 mm) phenocrysts of probable titanomagnetite are partly altered to leucoxene.

The matrix consists of an intimate mixture of fine-grained (30–50 µm) angular quartz grains, very fine grained (<10 µm) sericite and coarser (up to 200 µm) flakes of muscovite). Rounded grains of titanite are up to 100 µm in size. Several pinkish prismatic crystals of zircon were also found. In some quartz crystals were seen small (~150 µm) prisms of tourmaline and patches of sericite; tourmaline was also found in the vicinity of some titanomagnetite crystals.

The rock is most probably an altered granite porphyry (a dyke rock) or porphyritic rhyolite (effusive rock). It certainly is not a coarse granite.

Sample	***R1110473***		
Rock name	Quartz – feldspar porphyry		
Reference	S. McAvaney		
Location	761527 mE	6365802 mN	GDA94

Petrography

A visual estimate of the modal mineral abundances:

Mineral	Vol %
Quartz phenocrysts	20
Altered feldspar phenocrysts	30
Groundmass	42
Opaque	5
Quartz vein	5

Quartz phenocrysts are round to sub-round/polygonal, occasionally embayed, and range in size from 1.5–4 mm. They contain oblong-shaped inclusions ranging in size from 0.1–0.5 mm, consisting of very fine grained sericite, presumably replacing feldspar, and opaques.

Altered feldspar phenocrysts are euhedral to subhedral and are composed of very fine grained sericite, and contain opaque inclusions.

The groundmass is composed of oblong quartz crystals typically 0.1 mm, and masses of very fine grained sericite, which is probably replacing feldspar. The quartz and feldspar was probably initially granular in texture. Opaques constitute ~10% of the groundmass, a proportion of which may be secondary. They occur in a cubic habit and subhedral and anhedral forms, ranging in size from 20 µm to 1 mm, but typically 0.2 mm.

A quartz vein, varying from 0.5–1.5 mm thick, dissects the porphyry. It is composed of individual quartz crystal ranging in size from 0.2–0.5 mm, typically with the longest length of the crystal orthogonal to the vein wall, possibly preserving a relict epithermal texture. A thin opaque vein ~0.2 mm thick also dissects the porphyry.

Sample	***R1110474***		
Rock name	Quartz – feldspar porphyry		
Reference	S. McAvaney		
Location	756520 mE	6357283 mN	GDA94

Petrography

A visual estimate of the modal mineral abundances:

Mineral	Vol %
Quartz phenocrysts	15
Altered feldspar phenocrysts	25
Haematite altered groundmass	60

Quartz phenocrysts are round to sub-round/polygonal, and range in size from 1.5–4 mm. They contain irregularly shaped inclusions ranging in size from 0.125–0.25 mm consisting of masses of very fine grained sericite, probably replacing feldspar, and opaques.

Altered feldspar phenocrysts are euhedral to subhedral, ranging in size from 2–6 mm. They are completely replaced by very fine grained sericite, and contain inclusions of opaques.

The groundmass consists of polygonal quartz crystals ranging in shape from 0.125–0.2 mm and masses of very fine grained sericite presumably replacing feldspar. The quartz and feldspar was probably initially granular in texture. Traces allanite crystals ranging in size from 0.2–0.3 mm and opaques also occur in the matrix. The groundmass has been partially replaced by patches of red–brown haematite.

4. Geochemical Data

Sample locations

Sample	Lithology	Stratigraphy	Easting (GDA94)	Northing (GDA94)
R1562778	Alkali feldspar granite	Mu2	757272	6364792
R1562779	Alkali feldspar granite	Mu2	757349	6364723
R1562780	Quartz-feldspar porphyry	Mu1	757723	6364860
R1562782	Quartz-phyric fine grained granophyric granite	Mu2	756640	6365798
R1562784	Feldspar-phyric porphyritic monzogranite	Mu3	756666	6362262
R1562785	Feldspar-phyric porphyritic monzogranite	Mu3	756616	6362256
R1562786	Feldspar-phyric porphyritic monzogranite	Mu3	756564	6361900
R1562787	Tourmaline-quartz vein			
R1562788	Feldspar-phyric porphyritic monzogranite	Mu3	756713	6362326
R1562789	Feldspar-phyric porphyritic monzogranite	Mu3	756729	6362403
R1562790	Microgranite	Mu3	756667	6362464
R1562792	Alkali feldspar microgranite	Mu4	755512	6361252
R1562795	Micro-syenogranite	Mu5	755862	6361486
R1562796	Micro-syenogranite	Mu5	756367	6361639
R1562797	Feldspar-phyric porphyritic monzogranite	Mu3	755992	6359316
R1562799	Alkali feldspar granite	Mu2	758342	6358470
R1562800	Quartz-feldspar porphyry	Mu1	758188	6358896
R1562801	Quartz-feldspar porphyry	Mu1	758215	6359085
R1562802	Microgranite	Mu1	758176	6359228
R1562803	Brecciated microgranite	Mu1	758263	6358703
R1562804	Quartz-feldspar porphyry with haematite veining	Mu1	758263	6358703
R1110473	Quartz-feldspar porphyry	Mu1	761527	6365802

Major elements

Major Element	Al_2O_3	CaO	Fe_2O_3	K2O	MgO	MnO	Na_2O	P_2O_5	SiO_2	TiO_2	LOI
Units	wt %	wt %	wt %	wt %	wt %	wt %	wt %	wt %	wt %	wt %	ppm
Method	IC4	IC4	IC4	IC4	IC4	IC4	IC4	IC4	IC4	IC4	GRAV7
Detection Limit	0.01	0.01	0.01	0.01	0.01	0.01	0.01	0.01	0.01	0.05	0.01
Sample No.											
R1562778	11.3	0.28	1.66	4.86	0.38	0.02	2.38	0.02	77.4	0.145	1.02
R1562779	11	0.37	2.09	6.05	0.15	0.02	1.87	<0.01	76.4	0.14	0.59
R1562780	14.5	0.09	5.23	4.85	0.52	0.03	0.08	0.09	68.9	0.445	2.6
R1562782	11.5	0.47	1.76	5.82	0.07	0.01	2.64	0.01	75	0.145	0.79
R1562784	12.7	0.39	4.87	6.24	0.43	0.03	2.1	0.14	68.4	0.605	1.15
R1562785	13.1	0.11	4.89	8.49	0.44	0.04	0.14	0.08	68.9	0.63	1.53
R1562786	12.9	0.41	4.39	6.59	0.61	0.05	2.04	0.15	69	0.625	1.07
R1562787	14.7	0.48	13.9	0.11	3.13	0.02	1.48	0.04	56.4	0.145	1.63
R1562788	12.8	0.11	4.85	8.48	0.45	0.03	0.15	0.08	70.3	0.605	1.41
R1562789	13	0.12	4.72	8.06	0.52	0.02	0.14	0.07	69.7	0.585	1.66
R1562790	9.23	0.1	5.09	3.04	0.34	0.03	0.06	0.03	77.9	0.26	1.73
R1562792	11.9	0.11	0.96	8.74	0.28	0.03	0.14	0.03	75.5	0.29	1.19
R1562795	11.9	0.11	3.55	7.95	0.36	0.02	0.13	0.07	72.5	0.31	1.6
R1562796	11.5	0.13	2.94	8.11	0.3	0.02	0.16	0.04	74.2	0.29	1.19
R1562797	12.2	0.14	6.4	8.16	0.52	0.04	0.12	0.05	69.6	0.565	1.9
R1562799	11	0.09	1.79	3.03	0.06	0.01	0.2	0.06	80.7	0.265	1.88
R1562800	13.2	0.09	6.47	3.93	0.25	0.02	0.13	0.12	71.5	0.615	2.4
R1562801	12.3	0.11	2.9	3.72	0.19	0.01	0.12	0.06	77.4	0.56	2.06
R1562802	8.11	0.1	3.1	2.51	0.16	0.02	0.08	0.05	82.3	0.35	1.51
R1562803	7.67	0.09	15.5	2.37	0.23	0.02	0.12	0.07	70.1	0.24	1.73
R1562804	12.9	0.1	7.9	3.82	0.25	0.01	0.19	0.26	71.1	0.605	2.24
R1110473	14.2	0.05	4.38	4.85	0.33	0.03	0.07	0.05	70.1	0.32	2.27

Minor elements

Minor Element	Ag	As	Au	Ba	Be	Bi	Cd	Co	Cr
Units	ppm	ppm	ppb	ppm	ppm	ppm	ppm	ppm	ppm
Method	IC3M	IC3M	FA3E	IC4M	IC4M	IC3M	IC3M	IC3M	IC4
Detection Limit	0.1	0.5	1	10	0.5	0.1	0.1	0.2	20
Sample No.									
R1562778	<0.1	4	<1	350	6.5	0.4	<0.1	1.4	<20
R1562779	0.1	5	<1	185	6	0.4	<0.1	1.2	<20
R1562780	0.1	3	1	240	4	0.2	<0.1	1.7	<20
R1562782	<0.1	9	<1	140	6.5	0.4	<0.1	0.7	<20
R1562784	0.1	3.5	<1	1000	5	0.6	<0.1	6	<20
R1562785	0.1	3	<1	1100	4	0.8	<0.1	3.8	<20
R1562786	0.1	3.5	<1	1000	5.5	1	<0.1	7.5	20
R1562787	0.3	13	<1	45	9	0.2	<0.1	9	<20
R1562788	0.2	4	<1	1100	3.5	0.8	<0.1	2.4	<20
R1562789	0.2	3	<1	900	3.5	0.9	<0.1	3.3	<20
R1562790	0.2	3	<1	170	2.5	0.5	<0.1	1.5	<20
R1562792	0.2	2.5	<1	1000	3.5	0.3	<0.1	1.8	<20
R1562795	0.2	4	<1	950	3.5	0.6	<0.1	2.6	<20
R1562796	0.2	3	<1	950	3	0.9	<0.1	1.2	<20
R1562797	<0.1	4.5	<1	1150	3	0.6	<0.1	2.7	<20
R1562799	<0.1	5	<1	260	2	0.1	<0.1	0.4	<20
R1562800	0.1	5.5	<1	490	3	1.3	<0.1	5	<20
R1562801	<0.1	4.5	<1	250	3.5	0.2	<0.1	1.5	<20
R1562802	<0.1	3	<1	240	3	0.2	<0.1	1.3	20
R1562803	0.2	9.5	3	600	3	1.5	<0.1	1.8	20
R1562804	0.1	8	<1	600	3	0.2	<0.1	0.7	<20
R1110473	0.2	3	<1	280	3.5	1.3	<0.1	2.7	<20

Minor Element	Cs	Cu	Ga	Hf	In	Mo	Nb	Ni	Pb
Units	ppm	ppm	ppm	ppm	ppm	ppm	ppm	ppm	ppm
Method	IC3M	IC3M	IC3M	IC4M	IC3M	IC3M	IC4M	IC3M	IC3M
Detection Limit	0.1	0.5	0.1	1	0.05	0.1	10	2	0.5
Sample No.									
R1562778	2.6	7	23.5	4	<0.05	3.4	30	<2	6.5
R1562779	2.7	7.5	22	4	<0.05	0.6	40	<2	6.5
R1562780	2.3	2	28	7	0.1	0.3	25	2	5
R1562782	3.1	4	24	4	<0.05	0.8	55	<2	7.5
R1562784	1.9	78	22.5	7	<0.05	7.5	15	6	6.5
R1562785	2.5	11.5	21.5	8	<0.05	1.7	25	5	5
R1562786	1.9	14	23	7	<0.05	6.5	15	5	10
R1562787	<0.1	6.5	36	<1	0.4	0.6	20	8	3
R1562788	2.6	12.5	21.5	11	0.05	1.5	35	4	6
R1562789	2.5	12	23	11	0.05	1.2	35	3	8.5
R1562790	1.3	6	19	5	0.05	2.1	50	2	3
R1562792	4.7	4.5	16	4	<0.05	1	25	<2	4
R1562795	4.2	13.5	17	5	<0.05	6	25	3	9
R1562796	2.2	10.5	18	5	0.05	2.3	30	<2	4.5
R1562797	3	10.5	19.5	8	0.05	2.4	30	4	7.5
R1562799	0.5	3.5	15.5	4	<0.05	4.5	55	<2	6.5
R1562800	1.3	3.5	22.5	11	0.05	3.4	35	2	5
R1562801	1.2	3	22	9	<0.05	1.9	40	<2	5
R1562802	1	3	13	3	<0.05	0.7	<10	<2	2.5
R1562803	1.7	4.5	16.5	3	0.35	10	15	<2	9
R1562804	1.6	3	23	10	0.1	8.5	40	<2	5
R1110473	1.4	9	22	6	0.1	3.1	20	<2	3.5

Minor Element	Pd	Pt	Rb	Sb	Sc	Se	Sn	Sr	Ta
Units	ppb	ppb	ppm	ppm	ppm	ppm	ppm	ppm	ppm
Method	FA3E	FA3E	IC4M	IC3M	IC4	IC3M	IC4M	IC4M	IC4M
Detection Limit	1	5	0.5	0.5	5	0.5	10	5	2
Sample No.									
R1562778	<1	<5	600	1	<5	<0.5	<10	32	6
R1562779	<1	<5	600	1	<5	<0.5	<10	12	6
R1562780	<1	<5	600	3	6	<0.5	10	34	3
R1562782	<1	<5	650	1.5	<5	<0.5	<10	14	7
R1562784	<1	<5	380	1	8	<0.5	<10	34	3
R1562785	<1	<5	550	1.5	8	<0.5	<10	24	3
R1562786	<1	<5	390	1	8	<0.5	<10	52	2
R1562787	<1	<5	7	1	<5	<0.5	1100	80	<2
R1562788	<1	<5	550	2	6	<0.5	10	30	4
R1562789	<1	<5	550	2.5	8	<0.5	15	28	4
R1562790	<1	<5	320	3.5	6	<0.5	20	10	7
R1562792	<1	<5	500	1.5	<5	<0.5	10	16	4
R1562795	<1	<5	480	1.5	6	<0.5	<10	24	4
R1562796	<1	<5	600	2	<5	<0.5	<10	16	5
R1562797	1	<5	490	2.5	8	<0.5	<10	22	3
R1562799	<1	<5	230	1.5	6	<0.5	25	105	6
R1562800	<1	<5	420	3.5	8	<0.5	20	40	5
R1562801	<1	<5	390	2	6	<0.5	<10	16	4
R1562802	<1	<5	270	1.5	<5	<0.5	<10	20	<2
R1562803	<1	<5	420	6.5	<5	<0.5	45	68	2
R1562804	<1	<5	600	4	8	<0.5	35	180	4
R1110473	<1	<5	650	1.5	<5	<0.5	10	50	4

Minor Element	Te	Th	Tl	U	V	W	Y	Zn	Zr
Units	ppm	ppm	ppm	ppm	ppm	ppm	ppm	ppm	ppm
Method	IC3M	IC3M	IC3M	IC3M	IC4	IC3M	IC3M	IC3M	IC4
Detection Limit	0.2	0.02	0.1	0.02	20	0.1	0.05	0.5	20
Sample No.									
R1562778	<0.2	96	0.9	27.5	<20	2.3	34.5	9	190
R1562779	<0.2	115	1.1	15.5	<20	1.9	66	6.5	180
R1562780	<0.2	72	0.9	3.5	20	14	9.5	12.5	380
R1562782	<0.2	125	1.1	32.5	<20	1.3	38.5	6	170
R1562784	<0.2	54	0.9	12	30	3.7	56	25	420
R1562785	<0.2	50	1.4	9.5	30	8.5	43.5	12.5	450
R1562786	<0.2	48	1.1	11	40	2.8	47	32	440
R1562787	<0.2	25	<0.1	2.7	20	2.9	30.5	8.5	<20
R1562788	<0.2	52	1.4	10	30	7	36	14	450
R1562789	0.3	50	1.3	13.5	30	10.5	33.5	17	460
R1562790	<0.2	25	0.6	2.7	<20	17.5	10.5	15	170
R1562792	<0.2	22	1.1	3.5	<20	6	23.5	8.5	200
R1562795	<0.2	46	1.3	7.5	<20	5.5	24	14	220
R1562796	<0.2	45.5	1.3	6	<20	13.5	34.5	7	210
R1562797	<0.2	46	1.4	8	30	10.5	34.5	17	420
R1562799	<0.2	56	0.5	1.05	<20	16.5	6.5	6	170
R1562800	0.5	54	0.8	3.8	30	11.5	8	11	460
R1562801	<0.2	68	0.9	2.9	<20	10.5	11.5	12.5	440
R1562802	<0.2	20	0.6	1.6	20	4.5	6.5	8.5	180
R1562803	0.3	18	0.7	4.1	20	220	3.5	9	150
R1562804	<0.2	66	1	2.1	30	26.5	8.5	8	470
R1110473	<0.2	76	0.8	1.85	<20	6.5	10	17	320

REE

Major Element	Ce	La	Dy	Er	Eu	Gd	Ho
Units	ppm	ppm	ppm	ppm	ppm	ppm	ppm
Method	IC3R	IC3R	IC3R	IC3R	IC3R	IC3R	IC3R
Detection Limit	0.5	0.5	0.02	0.05	0.02	0.05	0.02
Sample No.							
R1562778	84	44.5	4.6	4.1	0.28	3	1
R1562779	190	135	7.5	7	0.52	5.5	1.75
R1562780	420	220	2.9	1.15	2.8	11	0.4
R1562782	130	70	4.3	4.8	0.3	2.2	1.05
R1562784	185	110	10.5	6.5	2.2	12.5	2
R1562785	330	195	10	5.5	2.5	15	1.7
R1562786	175	90	9	5.5	2	10.5	1.65
R1562787	78	54	5.5	3.5	0.68	5.5	1.05
R1562788	155	84	7.5	4.4	1.65	10	1.4
R1562789	190	105	7	4.2	1.65	9	1.25
R1562790	28.5	18	1.75	1.45	0.26	1.55	0.35
R1562792	155	92	4.5	2.7	1.05	7	0.83
R1562795	120	94	5	3.1	1	6	0.94
R1562796	160	86	6.5	4.5	1.15	7	1.3
R1562797	155	90	7.5	4.6	1.65	8	1.35
R1562799	130	180	1.25	1	0.5	1.45	0.25
R1562800	230	220	1.9	1.4	1.45	4.8	0.33
R1562801	110	110	2.4	2	0.97	3.5	0.48
R1562802	100	70	1.4	0.85	0.96	3.8	0.24
R1562803	60	39	0.75	0.55	0.47	1.45	0.14
R1562804	400	280	2.3	1.7	1.8	6	0.4
R1110473	125	100	2	1.35	0.71	3.1	0.38

Major Element	Lu	Nd	Pr	Sm	Tb	Tm	Yb
Units	ppm	ppm	ppm	ppm	ppm	ppm	ppm
Method	IC3R	IC3R	IC3R	IC3R	IC3R	IC3R	IC3R
Detection Limit	0.02	0.02	0.05	0.02	0.02	0.05	0.05
Sample No.							
R1562778	0.93	20	7	3.2	0.65	0.75	6.5
R1562779	1.5	46.5	18	6.5	1.1	1.2	10
R1562780	0.31	145	43.5	26	0.87	0.2	1.95
R1562782	1.3	23.5	9.5	3	0.55	0.9	8.5
R1562784	0.92	78	22	13.5	1.9	0.9	7
R1562785	0.8	120	36	19.5	2	0.75	6
R1562786	0.82	64	18.5	11.5	1.55	0.8	6
R1562787	0.56	22.5	7.5	4.6	0.93	0.5	4
R1562788	0.74	64	18	11	1.45	0.65	5.5
R1562789	0.74	74	22.5	12.5	1.3	0.65	5
R1562790	0.4	9	2.9	1.7	0.26	0.3	2.5
R1562792	0.45	62	18.5	9.5	0.89	0.4	3
R1562795	0.53	44.5	13.5	6.5	0.93	0.5	3.7
R1562796	0.76	50	16	8.5	1.15	0.7	5.5
R1562797	0.8	62	18.5	10	1.3	0.7	5.5
R1562799	0.27	64	24	6	0.21	0.2	1.75
R1562800	0.54	100	33.5	12	0.41	0.3	3.3
R1562801	0.67	62	20	8.5	0.41	0.45	4.4
R1562802	0.24	42	12.5	7	0.33	0.2	1.5
R1562803	0.16	20.5	6.5	3	0.15	0.1	1
R1562804	0.79	120	42	15.5	0.54	0.4	4.5
R1110473	0.34	36	11	5.5	0.38	0.25	2.3

REFERENCES

Anderson, C.G., 1980. Magnetic and Gravity Interpretation on the Stuart Shelf. Australian Society of Exploration Geophysicists, Bulletin 11 (3), 115-120 pp.

Australian Selection Pty. Ltd., 1977. EL212 Cultana. Progress Reports to Licence Renewal for the Period 28/10/1975 - 27/10/77., PIRSA Open File Envelope 2658.

Barbarin, B., 1999. A Review of the Relationships between Granitoid Types, their Origins and their Geodynamic Environments. Lithos, 46: 605-626.

Barker, D.S., 1970. Compositions of Granophyre, Myrmekite and Graphitic Granite. Geological Society of America Bulletin, 81: 3339-3350.

Belperio, A., Flint, R.B. and Freeman, H., 2007. Prominent Hill: A Haematite-Dominated, Iron Oxide Copper-Gold System. Economic Geology, 102: 1499-1510.

Belperio, A. and Freeman, H., 2004. Common Geological Characteristics of Prominent Hill and Olympic Dam - Implications for Iron Oxide Copper-Gold Exploration Models. Australian Institute of Mining and Metallurgy Bulletin, Nov-Dec: 67-75.

Blissett, A.H.C., 1987. Geological Setting of the Gawler Range Volcanics, Geological Atlas Special Series, 1:500 000. South Australia Department of Mines and Energy.

Bonython, W.V., 1984. Geochemistry of the Rare Earth Elements: Meteorite Studies. In: P. Henderson (Editor), Rare earth element geochemistry. Elsevier, pp. 63-114.

Budd, A.R., 1997. The Metallogenic Potential of Australian Proterozoic Granites: Gawler Craton and Curnamona Province. Australian Geological Survey Organisation, 5.

Budd, A.R., 2006. The Tarcoola Goldfield of the Central Gawler Gold Province, and the Hiltaba Association Granites, Gawler Craton, South Australia, Australian National University, Canberra.

Burnham, C.W., 1985. Energy Release in Subvolcanic Environments: Implications for Breccia Formation. Economic Geology, 80: 1515 - 1522.

Collins, L.G., 1997. The Mobility of Iron, Calcium, Magnesium and Aluminium during K- and Si-metasomatism. ISSN 1526-5757. www.csn.edu/~vcgeo005/mobility.htm

Conor, C.H.H., 1995. Moonta-Wallaroo Region. An Interpretation of the Geology of the Maitland and Wallaroo 1:100 000 Sheet Areas, PIRSA Open File Envelope 8886.

Cowley, W.M., 1991. Beda Volcanics and Backy Point Formation of the Eastern Gawler Craton, Department of Mines and Energy South Australia. Report Book 90/16.

Cox, K.G., Bell, J.D. and Pankhurst, R.J., 1979. The Interpretation of Igneous Rocks. George Allen and Unwin, London.

Craton Resources, 2001. EL 2478 and EL 2481. Point Lowly and Sunset Hill. Annual and Final reports for the Period 8/1/98 to 7/1/2001, South Australia. Department of Primary Industries and Resources. Open File Envelope, 9596.

Crawford, A.R. and Forbes, B.G., 1969. The Geology of the Cultana 1:63 360 Map Area, South Australia Department of Mines. Report of Investigations 34.

Crawford, A.R. and Hiern, M.N., 1964. Cultana Map Sheet. Geological Atlas 1:63 360 Series, South Australia Geological Survey.

Creaser, R.A., 1989. The Geology and Petrology of Middle Proterozoic Felsic Magmatism of the Stuart Shelf, South Australia, Australian National University, Canberra.

Creaser, R.A., 1996. Petrogenesis of a Mesoproterozoic Quartz Latite-Granitoid Suite from the Roxby Downs area, South Australia. Precambrian Research, 79: 371-394.

Dalgarno, C.R., Johnson, J.E., Forbes, B.G. and Thomson, B.P., 1968. Port Augusta 1:250 000 Geological Atlas Series Map. Sheet SI/53-4. Geological Survey South Australia. .

Daly, S.J., Fanning, C.M. and Fairclough, M.C., 1998. Tectonic evolution and Exploration Potential of the Gawler Craton, South Australia. AGSO Journal of Australian Geology and Geophysics, 17: 145-168.

Davidson, G.J., Paterson, H., Meffre, S. and Berry, R.F., 2007. Characteristics and Origin of the Oak Dam East Breccia-hosted, Iron Oxide Cu-U-(Au) Deposit: Olympic Dam Region, Gawler Craton, South Australia. Economic Geology, 102: 1471-1498.

De la Roche, H., Leterrier, J., Granclaude, P. and Marchal, M., 1980. A Classification of Volcanic and Plutonic Rocks using R1, R2-Diagram and Major Element Analyses - Its Relationships with Current Nomenclature. Chemical Geology, 29: 183-210.

Debon, F. and Le Fort, P., 1983. A Chemical-Mineralogical Classification of Common Plutonic Rocks and Associations. Transactions of the Royal Society of Edinburgh, Earth Sciences, 73: 135-149.

Dunham, A.C., 1965. The Nature and Origin of the Groundmass Textures in Felsites and Granophyres from Rhum, Inverness-shire. Geological Magazine, 102: 8-22.

Eagle Bay Resources, 2008. 4.1 Cultana Joint Venture EL 3547 (formerly ELA 105/2000) Whyalla South Australia - The Army Training Area (EBR 75%, Minotaur 25%). http://www.eaglebayresources.com.au/projects/overview.phtml

Eklund, O. and Shebanov, A.D., 1999. The Origin of Rapakivi Texture by Sub-isothermal Decompression. Precambrian Research, 95: 129-146.

Elders, W.A., 1966. Mantled feldspars from the Granites of Wisconsin. J Geol, 76.

Fairclough, M.C., 2005. Geological and Metallogenic Setting of the Carrapateena FeO-Cu-Au Prospect - a PACE Success Story. MESA Journal, 38: 4-7.

Fairclough, M.C. and Cowden, I., 1998. Review of Exploration and Mineral Potential. Myall Creek Project. EL2517 and ELA75/98. Gawler Craton and Stuart Shelf, South Australia, PIRSA Open File Envelope 9621.

Fanning, C.M., 1990. Single grain U-Pb zircon dating of a porphyritic volcanic from the Cultana complex, PRISE Report. Research School of Earth Sciences, Australian National University.

Fanning, C.M., Flint, R.B., Parker, A.J., Ludwig, K.R. and Blissett, A.H., 1988. Refined Proterozoic Evolution of the Gawler Craton, South Australia, through U-Pb zircon Geochronology. Precambrian Research, 40-41: 363-386.

Fanning, C.M., Reid, A.J. and Teale, G.S., 2007. A Geochronological Framework for the Gawler Craton, South Australia. South Australia Geological Survey. Bulletin 55.

Ferris, G.M. and Schwarz, M.P., 2003. Proterozoic Gold Province of the Central Gawler Craton. MESA Journal, 30: 4-12.

Flint et al, 1993. Mesoproterozoic. In: J.F. Drexel, W.V. Preiss and A.J. Parker (Editors), The Geology of South Australia. Vol 1, the Precambrian. South Australia Geological Survey, Bulletin 54.

Forbes, B.G. and Richards, E.F., 1975. Regional Geological Mapping and Cartographic Procedures. Mineral Resources Review, 137: 91-103.

Frost, B.R., Barnes, C.G., Collins, W.J., Arculus, R.J., Ellis, D.J. and Frost, C.D., 2001. A Geochemical Classification for Granitic Rocks. Journal of Petrology, 42: 2033-2048.

Gates, R.M., 1953. Petrogenetic Significance of Perthite. Geol Soc Am Mineral, 52: 55-69.

Geological Survey of South Australia, 1983. Geological Map of South Australia, 1:1 000 000. Geological Survey of South Australia.

Giles, C.W., 1980. A Comparative Study of Archaean and Proterozoic Felsic Volcanic Associations in Southern Australia, University of Adelaide.

Gostin, V.A., Hails, J.R. and Belperio, A., 1984. The Sedimentary Framework of Northern Spencer Gulf, South Australia. Marine Geology, 61: 111-138.

Haapala, I. and Ramo, O.T., 1999. Rapakivi Granites and Related Rocks: An Introduction. Precambrian Research, 95: 1-7.

Hand, M., Direen, N., Wade, B.P., Szpunar, M., Payne, J.L., Reid, A.J. and Barovich, K., 2007. Tectonics of the Olympic Dam Time Slice, South Australian Resources and Energy Investment Conference. Presentations, Abstracts and Posters.

Harding, R.R., 1969. Catalogue of Age Determinations on Australian rocks, 1962-65, Bureau of Mineral Resources, Australia. Report 117.

Hawkes, J., 1967. Rapakivi texture in the Dartmoor granite. Ussher Soc Proc, 1: 270-271.

Haynes, D.W., 1995. Olympic Dam Ore Genesis: A Fluid-Mixing Model. Economic Geology, 90: 281-307.

Hibbard, M.J., 1979. Synneusis Stacking of Plagioclase and the Mantling of Alkali Feldspar. Geological Society of America, Abstracts with Programs, 11: 84.

Hibbard, M.J., 1981. The Magma Mixing Origin of Mantled Feldspars. Contributions to Mineralogy and Petrology, 76: 158-170.

Holmquist, P.J., 1901. Rapakivistroktur och Granitetruktur. Geol Foren Forh, 23: 150-161.

Hutchison, R.M., 1956. Structure and Petrology of the Enchanted Rock Batholith, Llana and Gillespie counties, Texas. Geol Soc Am Bull, 67: 763-806

Johnson, J.P. and McCulloch, M.T., 1995. Sources of Mineralising Fluids for the Olympic Dam Deposit (South Australia): Sm-Nd Isotopic Constraints. Chemical Geology, 121: 177-199.

Larsen, E.S., Irving, J., Gonyer, F.A. and Larsen, F.S., 1938. Petrologic Results of a Study of the Minerals from the Tertiary Volcanic Rocks of the San Juan region, Colorado. American Mineralogist, 23: 227-257.

Lowder, G.G., 1973. The Geochronology of the Younger Granites of the Gawler Block and its Northwest Margin. Amdel Progress Report No.12 to 31st January 1973, PIRSA Open File Envelope, pp. 205-232.

Lowenstern, J.B., Clynne, M.A. and Bullen, T.D., 1997. Comagmatic A-Typle Granophyre and Rhyolite from the Alid Volcanic Center, Eritrea, Northeast Africa. Journal of Petrology, 38: 1707-1721.

Mason, M.G., 1980. Myall Creek Copper Prospect. Mineral Resources Review, 151: 58-64.

Mason, M.G., Thomson, B.P. and Tonkin, D.G., 1978. Regional Stratigraphy of the Beda Volcanics, Backy Point Beds and Pandurra Formation on the Southern Stuart Shelf, South Australia. Geological Survey of South Australia Quarterly Geological Notes, 66: 2-9.

Mathur, R., Marschik, R., Ruiz, J., Mumizaga, F., Leveille, R.A. and Martin, W., 2002. Age and Mineralisation of the Candelaria Fe Oxide Cu-Au Deposit and the Origin of the Chilean Iron Belt, Based on Re-Os Isotopes. Economic Geology, 97.

McDonough, W.F., Sun, S., Ringwood, A.E., Jagoutz, E. and Hofmann, A.W., 1992. K, Rb and Cs in the Earth and Moon and the Evolution of the Earth's Mantle. Geochimicia et Cosmochimica Acta. Ross Taylor Symposium Volume.

Middlemost, E.A.K., 1985. Magmas and Magmatic rocks: An Introduction to Igneous Petrology. Longman, London.

Nekvasil, H., 1991. Ascent of Felsic Magmas and Formation of Rapakivi. American Mineralogist, 76: 1279-1290.

Oliver, N.H.S., Cleverley, J.S., Mark, G., Pollard, P.J., Fu, B., Marshall, L.J., Rubenach, M.J., Williams, P.J. and Baker, T., 2004. Modelling the Role of Sodic Alteration in the Genesis of Iron Oxide-Copper-Gold Deposits, Eastern Mount Isa Block, Australia. Economic Geology, 99: 1145-1176.

Olliver, J.G. and Nichol, D., 1978. Barite Deposits near Whyalla, Northern Eyre Peninsula. Mineral Resources Review, 142: 90-100.

Oreskes, N. and Einaudi, M.T., 1990. Origin of Rare Earth Element-Enriched Hematite Breccias at the Olympic Dam Cu-U-Au-Ag Deposit, Roxby Downs, South Australia. Economic Geology, 85: 1-28.

Oreskes, N. and Einaudi, M.T., 1992. Origin of Hydrothermal Fluids at Olympic Dam: Preliminary Results from Fluid Inclusions and Stable Isotopes. Economic Geology, 87: 64-90.

Parker, A.J., Daly, S.J., Flint, D.J., Flint, R.B., Preiss, W.V. and Teale, G.S., 1993. Palaeoproterozoic. In: J.F. Drexel, W.V. Preiss and A.J. Parker (Editors), The Geology of South Australia. Vol. 1, The Precambrian. South Australia, Geological Survey. Bulletin 54.

Parker, A.J., Fanning, C.M., Flint, R.B., Martin, A.R. and Rankin, L.R., 1988. Archaean - Early Proterozoic Granitoids, Metasediments and Mylonites of Southern Eyre Peninsula, South Australia. Specialist Group in Tectonics and Structural Geology, Field Guide 2. Geological Society of Australia Incorporated, Adelaide.

Parker, A.J., Preiss, W.V. and Rankin, L.R., 1993. Geological Framework. In: J.F. Drexel, W.V. Preiss and A.J. Parker (Editors), The Geology of South Australia. Vol. 1, The Precambrian. South Australia Geological Survey, Bulletin 54.

Parkin, L.W., 1969. Handbook of South Australian Geology. Geological Survey of South Australia.

Preiss, W.V.C., 1987. The Adelaide Geosyncline - Late Proterozoic Stratigraphy, Sedimentation, Palaeontology and Tectonics. Bulletin 53. Geological Survey South Australia.

Purvis, A.C., 2008. Pontifex and Associates Pty. Ltd. Mineralogical report No. 9230.

Reeve, J.S., Cross, K.C., Smith, R.N. and Oreskes, N., 1990. Olympic Dam Copper-Uranium-Gold-Silver Deposit. In: F.E. Hughes (Editor), Geology of the Mineral Deposits of Australia and Papua New Guinea. The Australian Institute of Mining and Metallurgy, Melbourne, pp. 1009-1035.

Reynolds, L.J., 2001. Geology of the Olympic Dam Cu-U-Au-Ag-REE Deposit. MESA Journal, 23: 4-11.

Rollinson, H., 1993. Using Geochemical Data: Evaluation, Presentation and Interpretation. Harlow, Essex, England.

Serem Australia Pty Ltd, 1971. Cultana. Porphyry Copper Mineralisation Potential. Research Progress Reports for the Period 9/4/1970 to 17/4/1971., PIRSA Open File Envelope, 1722.

Sibenaler, X.P., 1972. Geochemical Sampling of Granites for Tin. Mineral Resources Review, 136: 38-45.

Skirrow, R., 2008. 'Haematite-Group' IOCG-U Ore Systems: Tectonic Settings, Hydrothermal Characterisitcs and Cu-Au and U Mineralizing Processes. In: L. Corriveau and H. Mumin (Editors), Exploring for Iron Oxide Copper-Gold Deposits: Canada and Global Analogues, Shortcourse Notes, GAC-MAC-SEG-SGA 2008, Quebec City, 29-30th May 2008. Geological Association of Canada.

Skirrow, R., Bastrokov, E., Barovich, K., Fraser, G., Creaser, R.A., Fanning, C.M., Raymond, O. and Davidson, G.J., 2007. Timing of Iron Oxide Cu-Au-(U) Hydrothermal Activity and Nd Isotope Constraints on Metal Sources in the Gawler Craton, South Australia. Economic Geology, 102: 1441-1470.

Skirrow, R., Fairclough, M.C., Budd, A.R., Lyons, P., Raymond, O., Milligan, P., Bastrokov, E., Fraser, G., Highet, L., Holm, O. and Williams, N., 2006. Iron Oxide Cu-Au (-U) Potential Map of the Gawler Craton, South Australia (First Edition), 1:500 000 scale. Geoscience Australia, Canberra.

South Australia Department of Mines, 1972. Geochemical Exploration Section, Exploration Services Division, Geological Survey Branch, South Australia, Department of Mines. Annual Report 1971-1972, pp. 64-66.

Stewart, D.B., 1956. Rapakivi Granite from Eastern Penobscot Bay, Maine. 20th International Geological Congress, Mexico, Proceedings, 11A: 293-320.

Stewart, K. and Foden, J., 2003. Mesoproterozoic Granites of South Australia, PIRSA Report Book 2003/15.

Stull, R.J., 1978. Mantled Feldspars from the Golden Horn Batholith, Washington. Lithos, 11: 243-249.

Stull, R.J., 1979. Mantled feldspars and Synneusis. American Mineralogist, 64: 514-518.

Sun, S., 1980. Lead Isotope Study of Young Volcanic Rocks from Mid-Ocean Ridges, Ocean Islands and Island Arcs. Philosophical Transactions of the Royal Society, A297: 409-445.

Terzaghi, R.D., 1940. The Rapakivi of Head Harbour Island, Maine. American Mineralogist, 25: 111-122.

Thomson, B.P., 1969. Precambrian Basement Cover - the Adelaide System. In: L.W. Parkin (Editor), Handbook of South Australian geology. Geological Survey of South Australia, pp. 49-83.

Thomson, B.P., Daily, B., Coats, R.P. and Forbes, B.G., 1976. Late Precambrian and Cambrian Geology of the Adelaide "Geosyncline" and Stuart Shelf, South Australia. 25th International Geological Congress. Excursion Guide 33A.

von Wolff, F., 1932. On Two Roof Pendants in the Wiborg Rapakivi Massif, Southeastern Finland. Geological Survey of Finland Bulletin, 272.

Wager, L.R., Vincent, E.A., Brown, C.M. and Bell, J.D., 1965. Marscoite and Related Rocks of the Western Red Hills Complex, Isle of Skye. Philosophical Transactions of the Royal Society of London, Series A, 257: 273-307.

Wahl, W., 1925. Die Gesteine des Wiborger Rapakivigebietes. Fennia, 45: 1-127.

Webb, A.W. and Coats, R.P., 1980. A Reassessment of the Age of the Beda Volcanics on the Stuart Shelf, South Australia, Department of Mines and Energy, South Australia. Report Book 80/6.

Webb, A.W. and Hörr, G., 1978. The Rb-Sr age and Petrology of a Flow from the Beda Volcanics. South Australia Geological Survey. Quarterly Geological Notes, 66: 10-13.

Webb, A.W., Thomson, B.P., Blissett, A.H., Daly, S.J., Flint, R.B. and Parker, A.J., 1986. Geochronology of the Gawler Craton, South Australia. Australian Journal of Earth Sciences, 33: 119-143.

Wingate, M.T.D., Campbell, I.H., Compston, W. and Gibson, G.M., 1998. Ion Microprobe U-Pb ages for Neoproterozoic Basaltic Magmatism in South-central Australia and Implications for the Breakup of Rodinia. Precambrian Research, 87: 135-159.